

ARTICLES

- Jänne, P.A., Gray, N. & Settleman, J. Factors underlying sensitivity of cancers to small-molecule kinase inhibitors. *Nat. Rev. Drug Discov.* **8**, 709–723 (2009).
- Carella, A.M. *et al.* New insights in biology and current therapeutic options for patients with chronic myelogenous leukemia. *Haematologica* **82**, 478–495 (1997).
- Schiller, J.H. *et al.* Comparison of four chemotherapy regimens for advanced non-small-cell lung cancer. *N. Engl. J. Med.* **346**, 92–98 (2002).
- Keedy, V.L. *et al.* American Society of Clinical Oncology provisional clinical opinion: epidermal growth factor receptor (EGFR) mutation testing for patients with advanced non-small-cell lung cancer considering first-line EGFR tyrosine kinase inhibitor therapy. *J. Clin. Oncol.* **29**, 2121–2127 (2011).
- Baccarani, M. *et al.* Chronic myeloid leukemia: an update of concepts and management recommendations of European LeukemiaNet. *J. Clin. Oncol.* **27**, 6041–6051 (2009).
- Wang, L., McLeod, H.L. & Weinshilboum, R.M. Genomics and drug response. *N. Engl. J. Med.* **364**, 1144–1153 (2011).
- Youle, R.J. & Strasser, A. The BCL-2 protein family: opposing activities that mediate cell death. *Nat. Rev. Mol. Cell Biol.* **9**, 47–59 (2008).
- Kuroda, J. *et al.* Bim and Bad mediate imatinib-induced killing of Bcr/Abl⁺ leukemic cells, and resistance due to their loss is overcome by a BH3 mimetic. *Proc. Natl. Acad. Sci. USA* **103**, 14907–14912 (2006).
- Aichberger, K.J. *et al.* Low-level expression of proapoptotic Bcl-2-interacting mediator in leukemic cells in patients with chronic myeloid leukemia: role of BCR/ABL, characterization of underlying signaling pathways, and reexpression by novel pharmacologic compounds. *Cancer Res.* **65**, 9436–9444 (2005).
- Kuribara, R. *et al.* Roles of Bim in apoptosis of normal and Bcr-Abl-expressing hematopoietic progenitors. *Mol. Cell. Biol.* **24**, 6172–6183 (2004).
- Cragg, M.S., Kuroda, J., Puthalakath, H., Huang, D.C. & Strasser, A. Gefitinib-induced killing of NSCLC cell lines expressing mutant EGFR requires BIM and can be enhanced by BH3 mimetics. *PLoS Med.* **4**, 1681–1689 (2007).
- Gong, Y. *et al.* Induction of BIM is essential for apoptosis triggered by EGFR kinase inhibitors in mutant EGFR-dependent lung adenocarcinomas. *PLoS Med.* **4**, e294 (2007).
- Costa, D.B. *et al.* BIM mediates EGFR tyrosine kinase inhibitor-induced apoptosis in lung cancers with oncogenic EGFR mutations. *PLoS Med* **4**, 1669–1679 (2007).
- Fullwood, M.J., Wei, C.L., Liu, E.T. & Ruan, Y. Next-generation DNA sequencing of paired-end tags (PET) for transcriptome and genome analyses. *Genome Res.* **19**, 521–532 (2009).
- Hillmer, A.M. *et al.* Comprehensive long-span paired-end-tag mapping reveals characteristic patterns of structural variations in epithelial cancer genomes. *Genome Res.* **21**, 665–675 (2011).
- Liu, J.W., Chandra, D., Tang, S.H., Chopra, D. & Tang, D.G. Identification and characterization of Bimgamma, a novel proapoptotic BH3-only splice variant of Bim. *Cancer Res.* **62**, 2976–2981 (2002).
- Adachi, M., Zhao, X. & Imai, K. Nomenclature of dynein light chain-linked BH3-only protein Bim isoforms. *Cell Death Differ.* **12**, 192–193 (2005).
- Ladd, A.N. & Cooper, T.A. Finding signals that regulate alternative splicing in the post-genomic era. *Genome Biol.* **3**, reviews0008 (2002).
- Carstens, R.P., McKeehan, W.L. & Garcia-Blanco, M.A. An intronic sequence element mediates both activation and repression of rat fibroblast growth factor receptor 2 pre-mRNA splicing. *Mol. Cell. Biol.* **18**, 2205–2217 (1998).
- Cheng, E.H. *et al.* BCL-2, BCL-X(L) sequester BH3 domain-only molecules preventing BAX- and BAK-mediated mitochondrial apoptosis. *Mol. Cell* **8**, 705–711 (2001).
- Huang, D.C. & Strasser, A. BH3-only proteins-essential initiators of apoptotic cell death. *Cell* **103**, 839–842 (2000).
- Kubonishi, I. & Miyoshi, I. Establishment of a Ph1 chromosome-positive cell line from chronic myelogenous leukemia in blast crisis. *Int. J. Cell Cloning* **1**, 105–117 (1983).
- Mahon, F.X. *et al.* Selection and characterization of BCR-ABL positive cell lines with differential sensitivity to the tyrosine kinase inhibitor ST1571: diverse mechanisms of resistance. *Blood* **96**, 1070–1079 (2000).
- Deininger, M.W., Goldman, J.M., Lydon, N. & Melo, J.V. The tyrosine kinase inhibitor CGP57148B selectively inhibits the growth of BCR-ABL-positive cells. *Blood* **90**, 3691–3698 (1997).
- Shah, N.P. *et al.* Transient potent BCR-ABL inhibition is sufficient to commit chronic myeloid leukemia cells irreversibly to apoptosis. *Cancer Cell* **14**, 485–493 (2008).
- Ly, C., Arechiga, A.F., Melo, J.V., Walsh, C.M. & Ong, S.T. Bcr-Abl kinase modulates the translation regulators ribosomal protein S6 and 4E-BP1 in chronic myelogenous leukemia cells via the mammalian target of rapamycin. *Cancer Res.* **63**, 5716–5722 (2003).
- Cragg, M.S., Harris, C., Strasser, A. & Scott, C.L. Unleashing the power of inhibitors of oncogenic kinases through BH3 mimetics. *Nat. Rev. Cancer* **9**, 321–326 (2009).
- La Rosée, P. & Hochhaus, A. Resistance to imatinib in chronic myelogenous leukemia: mechanisms and clinical implications. *Curr. Hematol. Malig. Rep.* **3**, 72–79 (2008).
- Paez, J.G. *et al.* EGFR mutations in lung cancer: correlation with clinical response to gefitinib therapy. *Science* **304**, 1497–1500 (2004).
- Lynch, T.J. *et al.* Activating mutations in the epidermal growth factor receptor underlying responsiveness of non-small-cell lung cancer to gefitinib. *N. Engl. J. Med.* **350**, 2129–2139 (2004).
- Shepherd, F.A. *et al.* Erlotinib in previously treated non-small-cell lung cancer. *N. Engl. J. Med.* **353**, 123–132 (2005).
- Kim, E.S. *et al.* Gefitinib versus docetaxel in previously treated non-small-cell lung cancer (INTEREST): a randomised phase III trial. *Lancet* **372**, 1809–1818 (2008).
- Park, K. & Goto, K. A review of the benefit-risk profile of gefitinib in Asian patients with advanced non-small-cell lung cancer. *Curr. Med. Res. Opin.* **22**, 561–573 (2006).
- Lu, Y., Liang, K., Li, X. & Fan, Z. Responses of cancer cells with wild-type or tyrosine kinase domain-mutated epidermal growth factor receptor (EGFR) to EGFR-targeted therapy are linked to downregulation of hypoxia-inducible factor-1 α . *Mol. Cancer* **6**, 63 (2007).
- Machida, K. *et al.* Characterizing tyrosine phosphorylation signaling in lung cancer using SH2 profiling. *PLoS ONE* **5**, e13470 (2010).
- Wu, J.Y. *et al.* Lung cancer with epidermal growth factor receptor exon 20 mutations is associated with poor gefitinib treatment response. *Clin. Cancer Res.* **14**, 4877–4882 (2008).
- Sasaki, H. *et al.* EGFR exon 20 insertion mutation in Japanese lung cancer. *Lung Cancer* **58**, 324–328 (2007).
- Gordon, P.M. & Fisher, D.E. Role for the proapoptotic factor BIM in mediating imatinib-induced apoptosis in a c-KIT-dependent gastrointestinal stromal tumor cell line. *J. Biol. Chem.* **285**, 14109–14114 (2010).
- Will, B. *et al.* Apoptosis induced by JAK2 inhibition is mediated by Bim and enhanced by the BH3 mimetic ABT-737 in JAK2 mutant human erythroid cells. *Blood* **115**, 2901–2909 (2010).
- Soda, M. *et al.* Identification of the transforming EML4-ALK fusion gene in non-small-cell lung cancer. *Nature* **448**, 561–566 (2007).
- Au, W.Y. *et al.* Chronic myeloid leukemia in Asia. *Int. J. Hematol.* **89**, 14–23 (2009).
- Faber, A. *et al.* BIM expression in treatment naive cancers predicts responsiveness to kinase inhibitors. *Cancer Discov.* **1**, 352–365 (2011).
- Cartegni, L., Chew, S.L. & Krainer, A.R. Listening to silence and understanding nonsense: exonic mutations that affect splicing. *Nat. Rev. Genet.* **3**, 285–298 (2002).
- López-Bigas, N., Audit, B., Ouzounis, C., Parra, G. & Guigo, R. Are splicing mutations the most frequent cause of hereditary disease? *FEBS Lett.* **579**, 1900–1903 (2005).
- Yano, S. *et al.* Hepatocyte growth factor induces gefitinib resistance of lung adenocarcinoma with epidermal growth factor receptor-activating mutations. *Cancer Res.* **68**, 9479–9487 (2008).
- Bivona, T.G. *et al.* FAS and NF- κ B signalling modulate dependence of lung cancers on mutant EGFR. *Nature* **471**, 523–526 (2011).
- Takeda, M. *et al.* De novo resistance to epidermal growth factor receptor-tyrosine kinase inhibitors in EGFR mutation-positive patients with non-small cell lung cancer. *J. Thorac. Oncol.* **5**, 399–400 (2010).
- Egle, A., Harris, A.W., Bouillet, P. & Cory, S. Bim is a suppressor of Myc-induced mouse B cell leukemia. *Proc. Natl. Acad. Sci. USA* **101**, 6164–6169 (2004).





ONLINE METHODS

Ethics committee approval. Clinical CML samples were obtained from patients seen at the Singapore General Hospital, the Akita University Hospital, the University of Malaya Medical Centre and the National University Cancer Institute, Singapore. German control samples were obtained from blood donors at the University Hospital of Bonn. Malay, Chinese and Indian control samples were derived from recent local population studies^{49,50}. Clinical NSCLC samples were obtained from patients seen at the National Cancer Centre, Singapore, the Toho University Omori Medical Center, Japan, the Aichi Cancer Center, Japan and the National University Cancer Institute, National University Health System, Singapore. Written informed consent and institutional review board approval at the participating institutions were obtained from all patients and normal individuals who contributed samples to this study.

DNA-PET sequencing and structural variation detection. DNA-PET sequencing and clustering of discordant PETs (dPETs) for structural variation detection has been described in Hillmer *et al.*⁵¹. DNA-PET libraries with 5-, 7- and 9-kb DNA fragments (Supplementary Table 2) were sequenced using the SOLiD platform (Applied Biosystems). The sequencing data from this study have been submitted to NCBI Gene Expression Omnibus (GEO) (<http://www.ncbi.nlm.nih.gov/geo/>) under accession number GSE28303 for the five patient samples and under accession number GSE26954 for K562. The genomic region that was covered by the 5' tags of a dPET cluster was defined as the 5' anchor, and the genomic region that was covered by the 3' tags of a cluster was defined as the 3' anchor. dPET clusters with anchor regions <500 bp were excluded from further analyses. The DNA-PET sequencing of K562 has been described earlier⁵¹. The same K562 dPET clusters used previously were also used in the present study, but the centromeric regions were not excluded here, dPET clusters with anchor regions <500 bp were excluded here (previously clusters with anchor regions <1,000 bp were excluded), and a new exclusion and filtering procedure was applied here (Supplementary Note and Supplementary Table 13).

Genotyping of the *BIM* polymorphic deletion. *Determination of patient genotype.* We extracted genomic DNA from either patients' peripheral blood (for both CML and NSCLC) or from formalin-fixed paraffin-embedded (FFPE) biopsy slides and blocks (for NSCLC). For DNA extracted from blood samples, we genotyped the deletion in the samples by a single PCR reaction using the primers 5'-AATACCACAGAGGCCACAG-3' and 5'-GCCTGAAGGTGCTGAGAAAG-3' and JumpStart RedAccuTaq LA DNA Polymerase (Sigma) with the following thermo cycling conditions: 96 °C for 30 s, (94 °C for 15 s, 60 °C for 60 s and 68 °C for 10 min) ×29 and 68 °C for 20 min. The resulting PCR products from the deletion (1,323 bp) and the wild-type (4,226 bp) alleles were analyzed on 1% agarose gels.

For DNA recovered from FFPE tissues, we performed two separate PCR reactions to determine the presence of the wild-type and deletion alleles. The wild-type allele was genotyped using the forward primer 5'-CCAATGGAAAAGGTTCA-3' and the reverse primer 5'-CTGTCATTTCTCCCACCAC-3'. The deletion allele was genotyped using the forward primer 5'-CCACCAATGGAAAAGGTTCA-3' and the reverse primer 5'-GGCACAGCCTCTATGGAGAA-3'. We performed PCR reactions using GoTaq Hot start Polymerase (Promega) with the following thermo cycling conditions: 95 °C for 5 min, (95 °C for 50 s, 58 °C for 50 s and 72 °C for 1 min) ×39 and 72 °C for 10 min. The PCR products for the deletion (284 bp) and the wild-type (362 bp) alleles were analyzed on a 2% agarose gel and were sequenced.

Determination of population frequency. We used Affymetrix Genome-Wide Human SNP Array 6.0 intensity data downloaded from the HapMap⁵² homepage (<http://snp.cshl.org/>) to infer the copy number of the deletion polymorphism in *BIM* for the HapMap samples. Two genotyped single nucleotide positions were located within the deletion: SNP_A-4195083 and CN_173550. The raw intensities of the two markers were used to call the copy number variation event using a Gaussian mixture model similar to the algorithm proposed by Korn and colleagues⁵³. Using this procedure, we predicted the copy number and, therefore, the presence or absence of the deletion in unrelated HapMap samples of European ($n = 60$), Yoruban ($n = 60$) and Chinese or Japanese ($n = 90$) origin. We then genotyped the deletion in the Chinese and Japanese samples for which we had available DNA ($n = 74$) by PCR as described above with the following

slight modifications of the thermo cycling conditions: 96 °C for 30 s, (94 °C for 15 s, 64 °C for 30 s and 68 °C for 5 min) ×12, (94 °C for 15 s, 60 °C for 30 s and 68 °C for 5 min) ×18 and 68 °C for 20 min. We used the PCR-based genotypes to refine the single-nucleotide intensity cutoffs for genotype calling in the European and Yoruban samples and used only the PCR-validated genotypes of the East Asian samples for frequency assessment.

To investigate further whether the deletion in the European population is at moderate frequency but has been missed by chance in the HapMap samples and to determine more precisely the deletion frequency in Asia, we genotyped by PCR assay 595 German, 600 Malay, 608 Chinese and 605 Indian samples.

Calculation of attributable fractions for the *BIM* deletion. To calculate the population attributable fraction (PAF) of treatment resistance in East Asian patients, we used $PAF = (f(OR - 1))/(f(OR - 1) + 1)$, where f is the frequency of deletion carriers among patients ($f = 0.133$), and OR is the odds ratio of the deletion carriers between patients being resistant and patients being sensitive to TKI treatment (OR = 2.94).

FISH. We used Vysis LSI (Locus specific identifier) BCR/ABL1 dual-fusion translocation probes (Abbott Molecular) for detecting *BCR-ABL1*. The LSI BCR probe is labeled with SpectrumGreen, and the LSI ABL1 probe is labeled with SpectrumOrange. We treated cells with 0.75 M KCl for 15 min at 37 °C. After fixation, we dropped the nuclei on slides for FISH according to the manufacturer's instructions with slight modifications. Briefly, we dehydrated the slides in a co-denaturated alcohol series for 3 min at 75 °C, which was followed by an overnight hybridization at 37 °C. We evaluated FISH signals in 200 interphase nuclei using a fluorescence microscope (Olympus BX60) under 1,000× magnification.

Cell lines, culture and chemicals. We purchased CML lines from American Type Culture Collection (ATCC) (MEG-01 and KU812), the Japanese Collection of Research Bioresources (NCO2) and the German Collection of Microorganisms and Cell Cultures (KCL22, K562, KYO-1, JK1, BV173 and NALM1). NSCLC cells (PC9 and HCC2279) were a gift from P. Koeffler. We cultured cells in RPMI-1640 medium supplemented with penicillin/streptomycin, glutamine and 10% FBS and incubated them in a humidified incubator at 37 °C with 5% CO₂. Zinc-finger-nuclease-edited K562 and PC9 cells were generated and maintained in RPMI-1640 medium supplemented with penicillin/streptomycin, glutamine and 20% FBS. Drugs were dissolved in DMSO (50% for imatinib; 100% for gefitinib and ABT-737) and kept at -20 °C. We used 1 μM imatinib and 0.5 μM gefitinib for all experiments, unless otherwise indicated. The treatment time was 12 h (Figs. 2g and 3d), 24 h (Figs. 2h-j and 4) or 48 h (Fig. 3e-i).

Real-time PCR analysis of exon-specific *BIM* transcripts. We extracted total cellular RNAs using the RNeasy Mini Kit (Qiagen). RNA was reverse transcribed using Superscript III First-Strand Synthesis System (Invitrogen) and quantitatively assessed using the iQ5 Multicolor Real-Time Detection System (Bio-Rad) with a total reaction volume of 25 μl. Primers were annealed at 59 °C for 20 s, and the amplicon was extended at 72 °C for 30 s. The total number of cycles quantified was 40. Transcript levels of β-actin or exon 2A of *BIM* were used to normalize between samples. The following primers were used: *BIM* exon 2A (forward: 5'-ATGGCAAAGCAACCTTCTGTATG-3'; reverse: 5'-GGCTCTGTCTGTAGGAGGT-3'), *BIM* exon 3 (forward: 5'-CATGGTAGTCATCCTAGAGG-3'; reverse: 5'-GACAAAATGCTCAAGGAGAGG-3'), *BIM* exon 4 (forward: 5'-TTCCATGAGGCAGGCTGAAC-3'; reverse: 5'-CCTCCTGCATAGTAAGCGTT-3') and β-actin (forward: 5'-GGACTTCGAGCAAGAGATGG-3'; reverse: 5'-AGCACTGTGTTGGCGTACAG-3').

RT-PCR and sequencing of *BIM* transcripts. To assess whether the splicing of *BIM* exons 3 and 4 are indeed mutually exclusive, we performed RT-PCR and sequenced all *BIM* transcripts that were amplified. Total cellular RNA extraction and reverse transcription was performed using the method described above. We used the forward primer 5'-ATGGCAAAGCAACCTTCTGA-3' and the reverse primer 5'-TCAATGCATTTCTCCACCA-3' to amplify all transcripts that contained exons 2 and 5. These primers were annealed at 57 °C for 30 s, and the amplicons were extended at 72 °C for 1 min. To amplify transcripts containing

exon 3, we used the forward primer 5'-TGACTCTCGGACTGAGAAACG-3' and the reverse primer 5'-CCAAAGCACAGTGAAGATCA-3'. These primers were annealed at 55 °C for 30 s, and the amplicons were extended at 72 °C for 30 s. All PCR products were cloned into pJET1.2/blunt vector (Fermentas) before they were sent for sequencing analysis.

Western blot. We used antibodies to the following to perform western blotting: BCR-ABL1 (#2802), pBCR-ABL1 (#2861), BIM (#2819), CRKL (#3182), pCRKL (#3181), CASPASE 3 (#9662), cleaved CASPASE 3 (#9661), STAT5A (#9310), pSTAT5A (#9359), ribosomal protein S6 (RPS6; #2317), pRPS6 (#2211), PARP (#9542), phospho-EGFR (Y1068,#2234) (all from Cell Signaling Technology), Flag-M2 clone and β -actin (#AC-15, Sigma). The antibody dilutions used were 1 in 1,000, except for pRPS6 (1 in 2,000) and β -actin (1 in 5,000). A BIM- γ -specific antibody was generated by a commercial entity (Open Biosystems). HRP-conjugated secondary antibodies were specific to rabbit (Sigma) or mouse IgG (Santa Cruz biotechnology). The protein bands on the membrane were visualized using the Western Lightning chemiluminescence reagent (PerkinElmer).

Minigene vector construction. We used the pI-12 splicing vector (a gift from M. Garcia-Blanco) to construct the minigene vectors pI-12-MUT and pI-12-WT, which contained and did not contain the deletion polymorphism, respectively. Briefly, BIM exon 4, together with a 659-bp sequence upstream of exon 4, was amplified from KCL22 genomic DNA using forward primer 5'-GCCGCTCGAGTCTCTCCATGTGGTGTGTTG-3' and reverse primer 5'-GCCGAAGCTTCCTCCTGCATAGTAAGCGT-3'. The PCR product was subcloned into the XhoI and HindIII sites in the pI-12 plasmid to generate an intermediate vector. BIM exon 3 and the upstream region with and without the deletion polymorphism were amplified from KCL22 genomic DNA using forward primer 5'-GCCGATATCATGGAAGGAAGTACCTGGTG-3' and reverse primer 5'-GCCGATCGATGTAGGAACTGGGTGAATGGC-3'. The two PCR products (4,500 bp and 1,597 bp) were subcloned into the EcoRV and ClaI sites in the intermediate vector to obtain the pI-12-WT and pI-12-MUT constructs. The ratios of exon 3 to exon 4 transcripts in the transfected cells were obtained by qPCR using specific primers for the U-E3 and U-E4 transcripts. Transcript levels were normalized to the adenovirus exon sequence (U). The following primers were used: adenovirus exon (forward: 5'-CGAGCTCACTCTCTCCGC-3'; reverse: 5'-CTGGTAGGGTACCTCGCA-3'), U-E3 transcript (forward: 5'-CGAGCTCACTCTCTCCGC-3'; reverse: 5'-CTCTAGGATGACTACTGGTAGGGT-3') and U-E4 transcript (forward: 5'-CGAGCTCACTCTCTCCGC-3'; reverse: 5'-CCTCATGGAAGCTGGTAGGGT-3').

siRNA knockdown of E3-containing BIM transcripts. siRNAs against E3-containing BIM transcripts (BIM- γ siRNA1: 5'-CCACCAUAGUCAAGAUACA-3'; BIM- γ siRNA2: 5'-CAGAACAACUCAACCACAA-3') and negative control siRNA (ON-TARGETplus Non-targeting siRNA #1) were purchased from Dharmacon Inc (Lafayette). Nucleofection was performed on KCL22 cells using Nucleofector Solution V (Lonza) in the presence of siRNAs.

Determination of protein stability and apoptotic activity of different BIM isoforms. We cloned the complementary DNA of different BIM isoforms (BIMEL, BIML, BIMS and BIM- γ ; gifts from A. Vazquez) into the pcDNA3-FLAG3 vector (a gift from K. Itahana). We transfected 5 μ g of plasmid into KCL22 (Supplementary Fig. 2e) or K562 cells (Supplementary Fig. 3a,b,d) by nucleofection. To determine apoptotic activity, we used Annexin V-FITC and 7-AAD staining and flow cytometry. To determine the stability of the BIM- γ and BIML proteins, we treated transfected cells with 50 μ g/ml of cycloheximide 44 h after nucleofection. Then we harvested the cells at various time points after treatment (0, 0.5, 1, 3, 5 and 7 h), and we determined the stability of Flag-tagged BIM- γ or BIML by western blot using antibodies to the Flag epitope.

Creation of BIM deletion polymorphism by ZFNs. The ZFN was custom made by Sigma-Aldrich CompoZr TM ZFN Technology with the following binding and cleavage sites: 5'-CCTTCCTGGAA-ctggga-ATAGTGGGTGAGATAGTG-3' (with the binding site in bold and the cleavage site not bolded). The cleavage site is located 551 bp downstream of the 5' end of the BIM deletion polymorphism region. The repair template contained only the two flanking homology arms but

not the BIM deletion polymorphism region. The repair template was constructed using a PCR strategy that used the KCL22 genomic DNA as a template and the forward primer 5'-CATAAATACCACAGAGGCCACAGC-3' (corresponding to a site 619 bp upstream from the 5' end of the BIM deletion polymorphism) and reverse primer 5'-CCCTCGAAGACACCTCTATTGGGAGGC-3' (corresponding to a site 743 bp downstream of the 3' end of the BIM deletion polymorphism). We subcloned the 1,362-bp PCR product into the vector pCR-Blunt II-TOPO (Invitrogen), and we confirmed the correct template by sequencing.

The repair template and ZFN-encoding plasmids were transfected into K562 cells using the protocol mentioned previously⁵⁴. To generate genome-edited cells, PC9 cells were seeded at a density of 2×10^5 cells per well in a six-well plate 1 d before transfection. The cells were transfected with the repair template (6 μ g) and ZFN-encoding plasmids (0.6 μ g each) using Eugene HD (Promega, USA). One day later, the transfected PC9 cells were arrested at the G2 phase for 18 h with 0.2 μ M vinblastine (Sigma, USA). The cells were released from G2 arrest by washing twice in PBS, re-plating in a new tissue culture plate and being allowed to recover for 72 h.

We isolated the genome-edited K562 and PC9 clones by dilution cloning. We diluted the transfected cells to a density of 2.5 cells/ml and seeded 200 μ l of the diluted cells into each well of a 96-well plate. Clones that successfully amplified from each well were harvested, and the genomic DNA was isolated using a Qiagen DNEasy kit (Hilden).

We screened for clones having the BIM deletion polymorphism by PCR using primers annealing to the BIM intronic region outside of the repair template, an approach that ensured the repair template would not be amplified. We used the forward primer 5'-GGCCTTCAACCACTATCTCAGTGCAATGG-3' (corresponding to a site 1,507 bp upstream from the 5' end of the BIM deletion polymorphism) and the reverse primer 5'-GGTTTCAGAGACAGAGCTGGGACTCC-3' (corresponding to a site 767 bp downstream of the 3' end of the BIM deletion polymorphism) for PCR.

ELISA-based DNA fragmentation detection and western blotting on genome-edited K562 and PC9 clones. The presence of mono- and oligo-nucleosomes in the apoptotic cells was detected using the Cell Death Detection ELISA (Roche), following the manufacturer's instructions. Genome-edited K562 cells were seeded at a density of 2×10^5 cells/ml. Five milliliters or 0.5 ml of cells were used for western blot or the apoptotic assay, respectively. The cells were harvested 48 h after treatment. Genome-edited PC9 cells were seeded at a density of 5×10^4 cells/ml. Ten milliliters or 0.5 ml of cells were used for western blot or the apoptotic assay, respectively. The cells were harvested 24 h after treatment.

Apoptosis assay in primary CML samples. We measured apoptosis in primary CML samples using the Annexin V-FITC kit (Beckman Coulter, IN) with propidium iodide, following the manufacturer's instructions. Statistical significance was determined using a one-tailed Wilcoxon rank sum test, as deletion-containing cells are expected to be more resistant than non-deletion-containing cells.

Trypan blue assay. PC9 and HCC2279 cells (5×10^5 and 1.6×10^5 cells, respectively) were seeded in triplicate and treated for 48 h. The cells were trypsinized, and the number of viable cells was determined by trypan blue exclusion.

Mutation analysis for EGFR. FFPE slides of lung tumors were deparaffined by washing the slides in xylene and absolute ethanol. Lung cancer regions from each slide were scraped and transferred into a 1.5-ml tube, and genomic DNA was extracted using a QIAamp FFPE Tissue kit (Qiagen). EGFR exons 18–21 were sequenced. Fifty nanograms of FFPE genomic DNA was amplified by PCR in a 20 μ l reaction volume containing 10 μ l of GoTaq hot start Taq colorless master mix (M5133, Promega) in the following PCR conditions: 95 °C for 5 min, DNA amplification for 35 cycles at 95 °C for 50 s, 58 °C for 50 s, 72 °C for 60 s and a final extension at 72 °C for 10 min. The PCR primers used were: exon 18 (forward: 5'-TGGCACTGCTTCCAGCATGG-3'; reverse: 5'-CTCCCCACAGACCATGAGAGG-3'), exon 19 (forward: 5'-ATC ACTGGGCAGCATGTGGCA-3'; reverse: 5'-CCTGAGGTTTCAGAGCCATGGAC-3'), exon 20 (forward: 5'-CATGCGAAGCCCACTGACGTG-3'; reverse: 5'-GCATGTGAGGATCCTGGCTC-3') and exon 21 (forward: 5'-GATCTGTCCCTCACAGCAGG-3'; reverse: 5'-GGTGTCTCAGAAAATGCTGG

CTG-3'). PCR products were purified by Exonuclease I (M0293L, New England Biolabs) and Shrimp Alkaline Phosphatase (Promega) treatments. Purified PCR products were sequenced in the forward and reverse directions using the ABI PRISM BigDye Terminator Cycle Sequencing Ready Reaction kit (Version 3) on an ABI PRISM 3730 Genetic Analyzer (Applied Biosystems, Foster City, California). Chromatograms were analyzed by SeqScape V2.5 and manual review.

Statistical analysis for PFS of patients with EGFR NSCLC. The primary endpoint in this study was to examine the effect of the *BIM* deletion polymorphism on the PFS of patients with EGFR-NSCLC from East Asian countries who were treated with EGFR TKIs. We calculated the PFS from the initiation of EGFR TKI therapy until either tumor progression or death from any cause. Observations were censored if TKI therapy was stopped because of side effects or if treatment was ongoing at the time of the analysis. We calculated the *P* values of the Kaplan-Meier test comparing survival curves using the Wilcoxon test. We used the *t* test and Fisher's exact test to test for differences between clinical characteristics of the *BIM*-deleted and wild-type populations. Using Cox proportional hazard regression analyses, univariate and multivariate hazard ratios were generated for the following factors: age, gender, histology, smoking history, type of EGFR mutation by exon and specific mutation, stage, first- or second-line TKI therapy,

race, country (Japan or Singapore), TKI (gefitinib or erlotinib) and ECOG status. The significance level for entering variables in a stepwise regression was 0.05. We used the SAS System for Windows Version 9.2 LIFETEST, TTEST and PHREG procedures to perform the calculations.

49. Foong, A.W. *et al.* Rationale and methodology for a population-based study of eye diseases in Malay people: the Singapore Malay eye study (SiMES). *Ophthalmic Epidemiol.* **14**, 25–35 (2007).
50. Lavanya, R. *et al.* Methodology of the Singapore Indian Chinese Cohort (SICC) eye study: quantifying ethnic variations in the epidemiology of eye diseases in Asians. *Ophthalmic Epidemiol.* **16**, 325–336 (2009).
51. Hillmer, A.M. *et al.* Comprehensive long-span paired-end-tag mapping reveals characteristic patterns of structural variations in epithelial cancer genomes. *Genome Res.* **21**, 665–675 (2011).
52. Frazer, K.A. *et al.* A second generation human haplotype map of over 3.1 million SNPs. *Nature* **449**, 851–861 (2007).
53. Korn, J.M. *et al.* Integrated genotype calling and association analysis of SNPs, common copy number polymorphisms and rare CNVs. *Nat. Genet.* **40**, 1253–1260 (2008).
54. Urnov, F.D. *et al.* Highly efficient endogenous human gene correction using designed zinc-finger nucleases. *Nature* **435**, 646–651 (2005).



REVIEW

ALKoma: A Cancer Subtype with a Shared Target

Hiroyuki Mano

ABSTRACT Anaplastic lymphoma kinase (ALK) is a receptor-type protein tyrosine kinase that is currently the focus of much attention in oncology. ALK is rendered oncogenic as a result of its fusion to NPM1 in anaplastic large cell lymphoma, to TPM3 or TPM4 in inflammatory myofibroblastic tumor, to EML4 in non-small cell lung carcinoma, and to VCL in renal medullary carcinoma. It is also activated as a result of missense mutations in neuroblastoma and anaplastic thyroid cancer. Whereas these various tumors arise in different organs, they share activated ALK, and a marked clinical efficacy with ALK inhibitors has already been shown for some of the tumors with ALK fusions. One of such compound, crizotinib, is now approved in the United States for the treatment of lung cancer positive for ALK rearrangement. I propose that tumors carrying abnormal ALK as an essential growth driver be collectively termed "ALKoma."

Significance: ALK acquires transforming ability through gene fusion or missense mutation in a wide range of human cancers. Some of these cancers, which I propose be collectively referred to as "ALKoma," may all be effectively treated with small compounds or antibodies targeted to activated ALKs. *Cancer Discov*; 2(6); 495–502. ©2012 AACR.

INTRODUCTION

Anaplastic lymphoma kinase (ALK) is a protein tyrosine kinase (PTK) that possesses a single transmembrane domain and consists of 1,620 amino acid residues in humans (Fig. 1; refs. 1, 2). The extracellular region of ALK contains 2 MAM (mepirin, A5 protein, and protein phosphatase μ) domains (3) and a putative ligand-binding domain. ALK is relatively isolated in the phylogenetic tree of the PTK superfamily, with its kinase domain sharing the highest sequence identity with that of the leukocyte receptor tyrosine kinase (LTK; 79% identity) and that of the proto-oncoprotein ROS1 (50% identity).

In the mouse, expression of ALK is prominent in the brain and peripheral nervous system of developing embryos, but it decreases rapidly after birth. In the adult human, ALK is expressed at a low level in the central nervous system but is not detected in other tissues (4). Given these expression profiles, ALK has been thought to play an important role in the development or orchestration of the nervous system.

Surprisingly, however, homozygous deletion of *Alk* in mice does not give rise to any apparent anomalies in morphology, internal organs, or fertility, suggesting that the gene is not essential for mouse development (5). A more detailed analysis of *Alk* knockout mice revealed an increase in the number of hippocampal progenitor cells in the brain and an enhanced performance in a test of novel object recognition. Another strain of such mice manifested increased ethanol consumption compared with heterozygous controls (6). These observations thus suggest that ALK may contribute to behavioral control in adult mice.

The structure of ALK, together with its expression pattern, suggests that it may function as a cell surface receptor for specific ligands that may regulate the proliferation or differentiation of neural cells. In the fruit fly, jelly belly (*jeb*) binds and activates an ortholog of ALK (7), but a mammalian ortholog of *jeb* has not been identified. The growth factors pleiotrophin and midkine have been proposed as candidate ligands for mammalian ALK (8, 9), but this notion remains controversial (10), leaving the biologic relevance of pleiotrophin and midkine unclear.

ALK first emerged in the field of oncology in 1994 as a result of the identification of its fusion to nucleophosmin (NPM1) in anaplastic large cell lymphoma (ALCL; Figs. 1 and 2; refs. 11, 12). The NPM1 portion mediates constitutive dimerization and consequent activation of the NPM1-ALK fusion protein (13). In addition to NPM1-ALK, various other ALK fusion proteins have now been identified in ALCL, including TFG-ALK, ATIC-ALK, and CLTC-ALK. The next disease linked to ALK was inflammatory myofibroblastic

Author's Affiliations: Division of Functional Genomics, Jichi Medical University, Tochigi; Department of Medical Genomics, Graduate School of Medicine, University of Tokyo, Tokyo, Japan; and CREST, Japan Science and Technology Agency, Saitama, Japan

Corresponding Author: Hiroyuki Mano, Division of Functional Genomics, Jichi Medical University, 3311-1 Yakushiji, Shimotsukeshi, Tochigi 329-0498, Japan. Phone: 81-285-58-7449; Fax: 81-285-44-7322; E-mail: hmano@jichi.ac.jp

doi: 10.1158/2159-8290.CD-12-0009

©2012 American Association for Cancer Research.

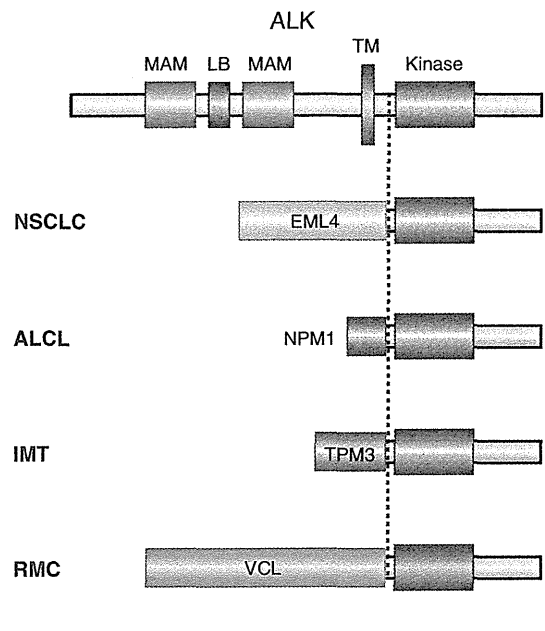


Figure 1. Structural organization of ALK and its fusion proteins. ALK is a receptor-type PTK with a single transmembrane (TM) domain as well as 2 MAM domains and a putative ligand-binding (LB) domain in the extracellular region. The intracellular region contains a kinase domain and is fused to EML4 in NSCLCs, to NPM1 in ALCLs, to TPM3 in IMTs, and to VCL in RMCs.

tumor (IMT), with increased expression of ALK and a rearranged *ALK* locus (chromosome band 2p23) being detected in a subset of IMT cases. A more detailed analysis identified *TPM3-ALK* and *TPM4-ALK* as fusion genes in IMT (Figs. 1 and 2; ref. 14). Further screening of IMT specimens revealed additional *ALK* fusions including *RANBP2-ALK* and *CARS-ALK*. Interestingly, some of these fusion genes, such as *TPM3/4-ALK* and *CLTC-ALK*, have been identified in both ALCLs and IMTs. The presence of *TPM3/4-ALK* was also reported in esophageal squamous cell carcinoma (15) and renal cancer (16).

In 2007, interest in ALK and the therapeutic potential of its specific inhibitors was boosted in response to the discovery of another fusion gene, *EML4-ALK*, this time in non-small cell lung carcinoma (NSCLC; ref. 17). Such interest was further increased the next year by the identification of activating point mutations in *ALK* in cases of neuroblastoma (18–21). In this review, I focus on activating genetic changes of *ALK* relevant to human cancer. Other aspects of *ALK* alterations (such as over-expression) in cancer have been elegantly reviewed elsewhere (22, 23).

EML4-ALK
EML4-ALK in NSCLC

Chronic myeloid leukemia (CML) is characterized by the presence of a fusion-type PTK, BCR-ABL1, that is generated as a result of a balanced chromosomal translocation, t(9;22). The remarkable therapeutic efficacy of the ABL1 inhibitor imatinib in individuals with this condition (24) suggested that targeting of the essential growth drivers in different types of cancer is a promising treatment strategy. To identify such growth drivers in clinical specimens, we developed a sensitive functional screening system based on retroviral cDNA expression libraries. The application of this approach to a lung adenocarcinoma specimen resulted in the discovery of *EML4-ALK* as a fusion-type oncogene (Figs. 1 and 2; ref. 17).

EML4 and *ALK* loci both map to the short arm of human chromosome 2 in opposite orientations and are separated by a distance of approximately 12 Mbp. A small inversion, inv(2)(p21p23), affecting both loci gives rise to the fusion gene. *EML4-ALK* was the first recurrent fusion-type oncogene in NSCLC, and, together with *ETS* fusions in prostate cancer (25), its existence argues against the previous notion that oncogenesis mediated by chromosome rearrangement is relatively specific to hematologic malignancies and sarcomas (rather than epithelial tumors).

EML4-ALK encodes a protein consisting of an amino-terminal portion of EML4 fused to the intracellular portion of ALK. *EML4-ALK* undergoes constitutive dimerization mediated through the coiled-coil domain of the EML4 portion and thereby acquires transforming ability in a manner

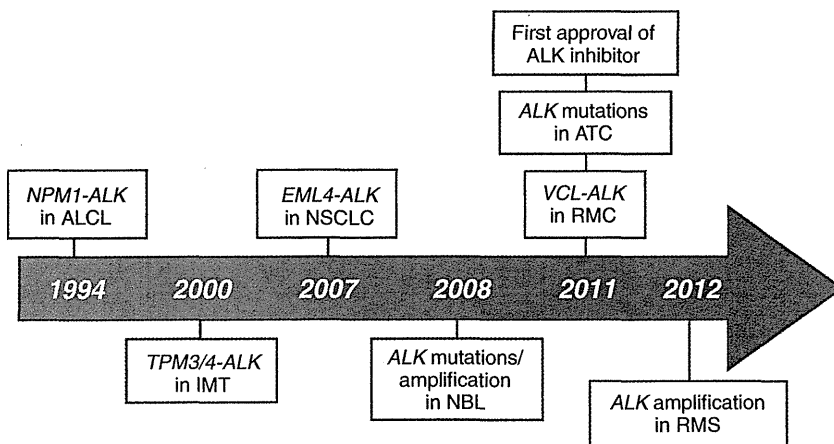


Figure 2. History of ALK in oncology. The first discovery of an oncogenic mutant of ALK was that of *NPM1-ALK* associated with ALCLs in 1994, which was followed by the identification of *TPM3/4-ALK* associated with IMTs, *EML4-ALK* associated with NSCLCs, mutated/amplified ALK associated with neuroblastoma (NBL), *VCL-ALK* associated with RMCs, mutated *ALK* associated with ATCs, and amplified *ALK* associated with rhabdomyosarcoma (RMS). Whereas several ALK inhibitors are currently in clinical trials, one such compound, crizotinib, was approved as a therapeutic drug for *ALK*-rearranged NSCLCs in 2011.

dependent on the associated upregulation of PTK activity. Indeed, several cell lines positive for *EML4-ALK* were found to be dependent on ALK catalytic activity for their proliferation (26, 27). Furthermore, transgenic mice that express *EML4-ALK* in lung type II alveolar cells manifest hundreds of adenocarcinoma nodules in both lungs soon after birth, and treatment of the animals with an ALK inhibitor results in the rapid clearance of these nodules (28). Such successful treatment of *EML4-ALK* transgenic mice with an ALK inhibitor was subsequently confirmed independently (29). These data suggested that *EML4-ALK* is the essential growth driver for NSCLC positive for this fusion kinase, and that targeting of ALK activity may therefore prove therapeutically effective in the clinic.

Clinicopathologic Features and Diagnosis of *EML4-ALK*-Positive Tumors

EML4-ALK is present in 3% to 6% of NSCLC cases (30–32). Of note, the clinical characteristics of patients with NSCLCs positive for *EML-ALK* are similar to those of such individuals who harbor activating mutations in the EGF receptor gene (*EGFR*): Both groups of patients thus tend to manifest an adenocarcinoma histology and to be non- or light smokers. However, the presence of *EML4-ALK* and that of *EGFR* or *KRAS* mutations are mutually exclusive, albeit with rare exceptions (33). Furthermore, whereas NSCLC with *EGFR* mutations is more prevalent in Asian populations than in Caucasians, no such ethnic differences have been reported for NSCLCs with *EML4-ALK*. With regard to pathologic characteristics, *EML4-ALK*-positive NSCLC has been found to contain signet-ring cells or to manifest a mucinous cribriform pattern (34–36), but other pathologic subtypes of NSCLCs also may harbor *EML4-ALK*. *EML4-ALK* may be infrequently present in other types of human cancers (16, 37).

The original *EML4-ALK* we identified resulted from ligation of intron 13 of *EML4* to intron 19 of *ALK* (17), but many other variants of the fusion gene have since been described. The vast majority of *ALK* translocations, including *EML4-ALK*, *NPM1-ALK*, and *TPM3-ALK*, involve intron 19 of *ALK*. Theoretically, ligation of *EML4* introns 1, 2, 6, 13, 18, 20, or 21 to intron 19 of *ALK* should generate an in-frame fusion at the mRNA level. Furthermore, given that exon 2 of *EML4* encodes the coiled-coil domain essential for *EML4-ALK* activation, all such fusions with the exception of that of *EML4*

intron 1 would be expected to generate an oncogenic kinase. Large-scale screening of clinical specimens has revealed that the original *EML4-ALK* variant (referred to as E13;A20 or variant 1) together with a variant in which intron 6 of *EML4* is fused to intron 19 of *ALK* (referred to as E6;A20 or variant 3; ref. 26) account for more than 90% of all *EML4-ALK*-positive cases of NSCLCs in Japan (M. Soda, personal communication), but many rare variants have also been identified (17, 26, 27, 30, 31, 34, 37, 38).

Importantly, *EML4* exons theoretically unable to undergo in-frame fusion to exon 20 of *ALK* may be involved in the generation of oncogenic *EML4-ALK* proteins. For instance, an *EML4-ALK* cDNA in which exon 14 of *EML4* is fused in-frame to the 13th nucleotide of *ALK* exon 20 has been identified (30). In addition, another variant in which the nucleotide located 19 bp upstream of the 3' end of *EML4* exon 15 is fused to that located 20 bp downstream of the 5' end of *ALK* exon 20 was described (27). It is therefore important that clinics adopt diagnostic techniques, such as those based on multiplex reverse transcription PCR (RT-PCR), that are able to capture all these variants of *EML4-ALK* reliably.

Currently, no single technique may be suitable for the analysis of all specimen types. Immunohistochemistry and FISH, for example, are applicable to formalin-fixed, paraffin-embedded (FFPE) tissue specimens (32, 34, 35) but may not be suitable for the analysis of sputum, pleural effusion, bronchial lavage fluid, or frozen tissue. Conversely, the latter specimen types are readily examined by RT-PCR (30), whereas the former ones may not be suitable for this technique. I thus propose that diagnostic tools for the detection of *EML4-ALK* should be selected on the basis of the available specimen types. FISH and immunohistochemistry should be applied to FFPE tissue samples, whereas multiplex RT-PCR is appropriate for the other specimen types.

Crizotinib

The first ALK inhibitor to enter clinical trials was crizotinib, which is also known as PF-02341066 and is actually a dual inhibitor for both ALK and MET kinases (Table 1; ref. 39). At the time of the discovery of *EML4-ALK*, crizotinib had already entered a phase I trial that mainly targeted digestive tract cancers positive for *MET* amplification. After the report of *EML4-ALK*, the phase I trial with crizotinib was expanded to include tumors positive for ALK rearrangement, and the drug soon proved as therapeutically efficacious for such tumors.

Table 1. ALK inhibitors under clinical trials or already approved

Inhibitor	Company	Trial phase	References
Crizotinib	Pfizer	Phase III (approved in United States, South Korea, and Japan)	39, 68
CH5424802	Chugai Pharmaceutical	Phase I/II	62
ASP3026	Astellas Pharma	Phase I	Not available
LDK378	Novartis	Phase I	Not available
AP26113	Ariad	Phase I/II	61

The response rate for crizotinib in patients with *ALK*-rearranged NSCLCs in the trial was shown to be 57%, with a disease control rate of up to 90% (32). Furthermore, the median overall survival for crizotinib treatment was not determinable within the follow-up period of 18 months (40). Comparison of crizotinib treatment with a historical control was further striking. Whereas the median overall survival was not achieved for patients who received crizotinib as a second- or third-line treatment, it was only 6 months for the *ALK*-rearranged control patients who received conventional chemotherapy in the second- or third-line setting.

While crizotinib can inhibit *MET* kinase activity and *MET* may become amplified in NSCLCs (41), there was no *MET* amplification present in the above *EML4-ALK*-positive cohort (32). Similarly, while *ROS1* tyrosine kinase is sensitive to crizotinib (42), a recent large-scale screening of gene fusions among NSCLC ($n = 1,529$) revealed a complete mutual exclusiveness between *ALK* and *ROS1* fusions (43). Furthermore, the mechanism for the insensitivity of *ALK* fusion-positive tumors to crizotinib has been mostly secondary mutations within the kinase domain of *EML4-ALK* (see below). These data evidence that crizotinib exerts its marked therapeutic efficacy in NSCLCs through specific suppression of *EML4-ALK* activity.

These observations clearly supported the clinical use of *ALK* inhibitors for the treatment of *EML4-ALK*-positive NSCLC. Indeed, on August 26, 2011, the U.S. Food and Drug Administration approved crizotinib as a treatment for *ALK*-rearranged NSCLCs. From the time of our first report of the identification of *EML4-ALK* in 2007, it took only 4 years for the first *ALK* inhibitor to be approved for use in the clinic, which is a record for cancer drug development (44).

OTHER *ALK* TRANSLOCATIONS IN EPITHELIAL TUMORS

Following the discovery of *EML4-ALK*, efforts have expanded to detect novel *ALK* fusions in epithelial tumors. Development of a sensitive immunohistochemical technique (intercalated antibody-enhanced polymer method, or iAEP) to stain *ALK* proteins in FFPE specimens led to the identification of several NSCLC samples that were positive with this approach but negative for *EML4-ALK* with multiplex RT-PCR (34). Further investigation of these specimens revealed the presence of another fusion of *ALK*, *KIF5B-ALK*. Similar to *EML4-ALK*, *KIF5B* contains dimerization motifs that play an essential role in the oncogenic activity of *KIF5B-ALK* and there are now known to be several variants of *KIF5B-ALK* (45). Togashi and colleagues reported still another *ALK* fusion, *KLC1-ALK*, in NSCLCs (46).

Yet another novel *ALK* fusion, *VCL-ALK*, was recently identified in a tumor of unclassified renal cell carcinoma with renal medullary carcinoma (RMC) characteristics that developed in a 16-year-old boy with sickle cell trait (47). *VCL-ALK* was also detected in RMCs isolated from a 6-year-old boy (48). RMC mostly affects young individuals and has a poor outcome, but the discovery of *VCL-ALK* has raised the possibility of effective treatment with an *ALK* inhibitor for patients who harbor this fusion gene. Furthermore, screening of tissue microarrays of renal cell carcinoma with the iAEP technique led to the detec-

tion of single cases each positive for *TPM3-ALK* or *EML4-ALK* (*E2;A20* variant; ref. 16).

ONCOGENIC POINT MUTATIONS IN *ALK* Neuroblastoma

Attempts by several groups to identify genes underlying neuroblastoma through different approaches (mapping of single-nucleotide polymorphisms for familial neuroblastoma and chromosome copy number analysis for sporadic neuroblastoma) resulted in the almost simultaneous identification of activating mutations within *ALK* (Figs. 2 and 3; refs. 18–21). About 10% of sporadic neuroblastoma cases harbor somatic nonsynonymous mutations within *ALK*, including K1062M, F1174L/C/I, F1245C/V/L, and R1275Q amino acid substitutions. On the other hand, a distinct but partially overlapping set of *ALK* mutations (T1087I, G1128A, R1275Q, and others) has been identified in familial neuroblastoma.

Importantly, these mutations do not confer equal transforming ability. The F1174L mutant, for instance, efficiently phosphorylates the signaling molecules *STAT3* and *AKT*, but not extracellular signal-regulated kinase (*ERK*)1/2, whereas the R1275Q mutant efficiently phosphorylates *ERK*1/2 but not *STAT3* (18). Knockdown experiments revealed that the growth of neuroblastoma cell lines was dependent to a greater extent on the F1174L mutant than on R1275Q (18, 20). The mutant *ALK* proteins thus contribute substantially to the transformation process in neuroblastoma, but the extent to which they do so varies among the mutation types.

These mutations also differentially affect the sensitivity of neuroblastoma to *ALK* inhibitors (49, 50), which may not be surprising given that point mutations within the kinase domain of *ALK* affect its 3-dimensional structure (including that of the inhibitor binding cleft) and thereby influence inhibitor binding. The F1174L mutant confers marked resistance to crizotinib in a cell-based assay (49, 50), suggesting that this amino acid substitution not only increases the enzymatic activity of *ALK* by changing the structure of the kinase domain but by doing so also affects the binding of *ALK* inhibitors.

The I1250T mutation of *ALK* was recently identified in an individual with neuroblastoma and was shown to abolish the activity of the enzyme (51). Each *ALK* mutation identified in neuroblastoma therefore needs to be assessed for how (or if) it contributes to carcinogenesis.

Anaplastic Thyroid Cancer

Nucleotide sequencing of *ALK* exons encoding the kinase domain in cell lines and fresh specimens of thyroid cancer (52) revealed novel missense mutations specifically in anaplastic thyroid cancer (ATC) samples (2 positive samples of 11). Each of the 2 identified amino acid substitutions (L1198F and G1201E) increased the enzymatic activity of *ALK* and induced the formation of transformed foci when introduced into mouse 3T3 cells, clearly indicating the activating nature of these mutations. It is thus likely that a subset of ATC and neuroblastoma cases share the same transforming gene, but it remains to be determined whether the *ALK* mutation profiles differ between the 2 disorders.

GENE AMPLIFICATION OF ALK

In addition to nonsynonymous mutations, *ALK* infrequently becomes amplified in neuroblastoma (21, 53). While its clinical relevance is yet to be clarified, *ALK* amplification frequently co-occurs with amplification of *MYCN* amplification, a known growth driver for this disorder, suggesting that *ALK* also contributes to carcinogenesis.

Recently, van Gaal and colleagues (54) have discovered frequent copy number gain of *ALK* in rhabdomyosarcoma accompanied with an increased level of ALK protein. In some cases, *ALK* copy number was even above 10. Interestingly, contrary to neuroblastoma, rhabdomyosarcoma with *ALK* amplification do not carry *MYCN* amplification. Such *ALK* anomaly is likely to be connected to carcinogenesis because *ALK* gain was associated with poor survival and the occurrence of metastases. In addition, van Gaal and colleagues also identified one case with ALK (D1225N) and 7 with *ALK* frameshift mutations of 43 rhabdomyosarcoma specimens, although clinical relevance of such mutations is yet to be examined.

RESISTANCE TO ALK INHIBITORS

Some *EML4-ALK*-positive NSCLC tumors are insensitive to initial treatment with ALK inhibitors, whereas others acquire resistance to these drugs after initial successful treatment. Information on the molecular mechanisms underlying such resistance remains limited.

The first insight into such resistance mechanisms was provided by analysis of an individual with *EML4-ALK*-positive NSCLC who initially showed a partial response to crizotinib treatment but underwent a rapid relapse after 5 months. *EML4-ALK* cDNA was amplified by PCR from tumor specimens obtained before the onset of treatment and after relapse, and it was then subjected to deep sequencing with a next-generation sequencer. Comparison of the 2 data sets resulted in the identification of 2 nonsynonymous mutations present only in the latter specimen. Interestingly, these 2 amino acid substitutions (C1156Y and L1196M) were found to independently confer resistance to crizotinib and other ALK inhibitors (55).

Neither C1156Y nor L1196M affects the enzymatic activity of *EML4-ALK*. NSCLC cells harboring either mutant might therefore be positively selected *in vivo* only in the presence of ALK inhibitors. Furthermore, Leu¹¹⁹⁶ is the "gatekeeper" site buried deeply within the ATP-binding pocket of ALK, with the corresponding sites of EGFR (Thr⁷⁹⁰) and BCR-ABL1 (Thr³¹⁵) being the most frequently mutated residues associated with gefitinib and imatinib resistance, respectively (56).

Examination of a similar *EML4-ALK*-positive individual who initially responded to crizotinib but later acquired resistance revealed the presence in post-relapse *EML4-ALK* cDNA of a mutation resulting in an L1152R substitution in the kinase domain (57). Another mutation conferring drug resistance (F1174L) was identified in a case of RANBP2-*ALK*-positive IMTs (58). Of note, F1174L is also one of the frequent amino acid substitutions identified in neuroblastoma (Fig. 3). Further extensive screening of crizotinib-resistant mutations among 18 relapsed patients revealed 4 secondary mutations (I151Tins, L1196M, G1202R, and S1206Y) within the kinase domain of *EML4-ALK*, all of which confer resistance to ALK

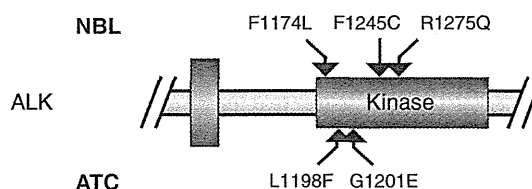


Figure 3. Missense mutations in ALKs. Activating mutations of ALKs are associated with familial and sporadic neuroblastoma (NBL). A different set of missense mutations is also associated with a subset of ATC tumors. Representative mutations for each disorder are shown according to their location in the kinase domain of ALK.

inhibitors (59). Such investigation further identified a high-level amplification of *EML4-ALK* in one patient, suggesting another mechanism (gene amplification) of drug insensitivity.

Another screening of *EML4-ALK*-positive tumors at a relapsed phase led to the identification of L1196M (in 2 of 14 resistant cases) and G1269A (in 2 cases) mutations accounting for the acquired drug resistance, and of gene amplification in 2 cases (60). Interestingly, in this cohort, some tumors lost *EML4-ALK* oncogene at the relapsed phase, but instead acquired activating *EGFR* or *KRAS* mutations. Whether such oncogenes other than *EML4-ALK* were present in a minor population of the original tumor or secondarily acquired during the crizotinib treatment remains elusive.

As of March 2012, 5 distinct ALK inhibitors are in clinical trials worldwide (Table 1), with some of these drugs showing inhibitory activity *in vitro* even with the gatekeeper mutant (61, 62). It will thus be of interest to determine whether treatment with such inhibitors results in the development of acquired resistance or not.

ALKOMA: A STEP TOWARD GENETIC INFORMATION-BASED CANCER CLASSIFICATION

Since the initial discovery of NPM1-*ALK* in 1994, our knowledge of the role of ALK in human cancer has increased markedly. We now recognize the contribution of ALK to an unexpectedly wide range of tumors, with *ALK* translocations underlying lymphoma, lung carcinoma, kidney cancer, and soft tissue tumors and *ALK* mutations being responsible for neuronal and thyroid cancer and *ALK* amplification frequently occurring in rhabdomyosarcoma.

Given that all ALK fusion kinases retain an intact ATP-binding pocket (where most ALK inhibitors bind), it is likely that ALK inhibitors will be effective against any tumor type that harbors such an ALK fusion (63, 64). From the standpoint of pharmaceutical companies, the fact that a single compound can serve as a magic pill for many different types of cancer in different organs is sufficiently compelling to warrant the development of such drugs even if the individual cancer types do not have a high incidence.

For neuroblastoma and ATC, however, the efficacy of an ALK inhibitor may be substantially influenced by the type or position of the missense mutation. However, given that ALK is a transmembrane protein, the mutant proteins may

be effectively targeted by antibodies (65), as is the case for other transmembrane proteins targeted by the antibodies rituximab and trastuzumab.

Genetic information was first integrated into the classification of hematologic malignancies. For instance, whereas acute myeloid leukemia (AML) had previously been divided into subgroups with distinct differentiation profiles (assessed by pathologic analyses), AML harboring *RUNX1-RUNX1T1*, *PML-RARA*, or *MLL* rearrangements is now defined as a distinct entity according to the current World Health Organization classification (66). Likewise, all-*trans* retinoic acid is highly effective only in the treatment of retinoic acid receptor alpha (encoded by *RARA*) fusion-positive AML, acute promyelocytic leukemia (APL). Similarly, ABL1 inhibitors are only used against *BCR-ABL1*-positive CML/acute lymphoblastic leukemia. It is likely that tumor cells of APL or CML are deeply addicted to the activity of PML-RARA or BCR-ABL1, respectively. Therefore, single reagents targeting individual oncoproteins have a profound therapeutic effect.

In the treatment of epithelial tumors, single EGFR inhibitors provide a high response rate to NSCLCs harboring activating *EGFR* mutations as well. Importantly, treatment with such EGFR inhibitors worsens the prognosis of NSCLC without *EGFR* mutations (67). Targeted drugs are, thus, likely to be highly effective only against tumors in which corresponding targets carry activating mutations and become “essential growth drivers” for the cancer. The definition of essential growth drivers for given oncogenes is difficult because treatment efficacy for cell lines *in vitro* does not always recapitulate that in clinics. For instance, while inhibitors against RAS or PIK3CA are able to suppress the growth of cancer cell lines, these compounds have failed to provide such efficacy in humans.

Therefore, significant response in patients by a monotherapy with a targeted drug should be a faithful indicator for the corresponding target to be the essential growth driver. Unfortunately, however, such clinically proven drivers are still few, but EML4-ALK is a newcomer to this growing list. Importantly, other ALK fusions, NPM1-ALK and RANBP2-ALK, are likely the essential growth drivers as well, because the crizotinib monotherapy has a profound therapeutic effect (63, 64). I propose that these tumors be collectively referred to as “ALKoma,” in which abnormal ALK plays an indispensable component in the carcinogenesis.

Interestingly, the term “ALKoma” encompasses multiple organs. NSCLCs, IMTs, and ALCLs were once regarded as completely distinct clinical entities affecting different organs. However, it is now known that a fraction of each of these cancer types shares activated ALK as the essential growth driver and such tumors can be targeted for treatment with ALK inhibitors (32, 63, 64). Because of the similar protein structure to that of EML4-ALK/NPM1-ALK/RANBP2-ALK, VCL-ALK in RMCs should be a good candidate for the next member of ALKoma. Data from ongoing clinical trials with crizotinib for neuroblastoma will also tell us whether activated ALK with nonsynonymous mutations is also a strong driver for this disorder. The term “ALKoma” has the advantage that it indicates the preferred treatment for the tumor. It is thus a good example of genetic information-based “beyond organ” cancer classification, many other examples of which may emerge in the future.

Disclosure of Potential Conflicts of Interest

H. Mano has commercial research grant from Astellas Pharma and Illumina Inc.; Ownership Interest (including patents); and serves as a scientific advisor for Pfizer Inc., Astellas Pharma, Chugai Pharmaceutical, and Daiichi Sankyo Co., Ltd., and is a CEO of CureGene Co., Ltd.

Author's Contributions

Conception and design: H. Mano

Analysis and interpretation of data (e.g., statistical analysis, biostatistics, computational analysis): H. Mano

Writing, review, and/or revision of the manuscript: H. Mano

Study supervision: H. Mano

Acknowledgments

The author apologizes to all the authors whose work could not be included in the manuscript owing to space constraints and also thanks the members of his laboratory as well as K. Takeuchi for their dedication and support.

Grant Support

This work was supported in part by a grant for Research on Human Genome Tailor-made from the Ministry of Health, Labor, and Welfare of Japan as well as by a Grant-in-Aid for Scientific Research on Priority Areas from the Ministry of Education, Culture, Sports, Science, and Technology of Japan.

Received January 6, 2012; revised April 20, 2012; accepted April 20, 2012; published OnlineFirst May 21, 2012.

REFERENCES

- Morris SW, Naeve C, Mathew P, James PL, Kirstein MN, Cui X, et al. ALK, the chromosome 2 gene locus altered by the t(2;5) in non-Hodgkin's lymphoma, encodes a novel neural receptor tyrosine kinase that is highly related to leukocyte tyrosine kinase (LTK). *Oncogene* 1997;14:2175-88.
- Iwahara T, Fujimoto J, Wen D, Cupples R, Bucay N, Arakawa T, et al. Molecular characterization of ALK, a receptor tyrosine kinase expressed specifically in the nervous system. *Oncogene* 1997;14:439-49.
- Beckmann G, Bork P. An adhesive domain detected in functionally diverse receptors. *Trends Biochem Sci* 1993;18:40-1.
- Pulford K, Lamant L, Morris SW, Butler LH, Wood KM, Stroud D, et al. Detection of anaplastic lymphoma kinase (ALK) and nucleolar protein nucleophosmin (NPM)-ALK proteins in normal and neoplastic cells with the monoclonal antibody ALK1. *Blood* 1997;89:1394-404.
- Bilsland JG, Wheelton A, Mead A, Znamenskiy P, Almond S, Waters KA, et al. Behavioral and neurochemical alterations in mice deficient in anaplastic lymphoma kinase suggest therapeutic potential for psychiatric indications. *Neuropsychopharmacology* 2008;33:685-700.
- Lasek AW, Lim J, Kliethermes CL, Berger KH, Joslyn G, Brush G, et al. An evolutionary conserved role for anaplastic lymphoma kinase in behavioral responses to ethanol. *PLoS One* 2011;6:e22636.
- Lee HH, Norris A, Weiss JB, Frasch M. Jelly belly protein activates the receptor tyrosine kinase Alk to specify visceral muscle pioneers. *Nature* 2003;425:507-12.
- Stoica GE, Kuo A, Aigner A, Sunitha I, Souttou B, Malerczyk C, et al. Identification of anaplastic lymphoma kinase as a receptor for the growth factor pleiotrophin. *J Biol Chem* 2001;276:16772-9.
- Stoica GE, Kuo A, Powers C, Bowden ET, Sale EB, Riegel AT, et al. Midkine binds to anaplastic lymphoma kinase (ALK) and acts as a growth factor for different cell types. *J Biol Chem* 2002;277:35990-8.
- Mathivet T, Mazot P, Vigny M. In contrast to agonist monoclonal antibodies, both C-terminal truncated form and full length form of Pleiotrophin failed to activate vertebrate ALK (anaplastic lymphoma kinase)? *Cell Signal* 2007;19:2434-43.

11. Morris SW, Kirstein MN, Valentine MB, Dittmer KG, Shapiro DN, Saltman DL, et al. Fusion of a kinase gene, ALK, to a nucleolar protein gene, NPM, in non-Hodgkin's lymphoma. *Science* 1994;263:1281-4.
12. Shiota M, Fujimoto J, Semba T, Satoh H, Yamamoto T, Mori S. Hyperphosphorylation of a novel 80 kDa protein-tyrosine kinase similar to Ltk in a human Ki-1 lymphoma cell line. *AMS3. Oncogene* 1994;9:1567-74.
13. Pulford K, Lamant L, Espinos E, Jiang Q, Xue L, Turturro F, et al. The emerging normal and disease-related roles of anaplastic lymphoma kinase. *Cell Mol Life Sci* 2004;61:2939-53.
14. Lawrence B, Perez-Atayde A, Hibbard MK, Rubin BP, Dal Cin P, Pinkus JL, et al. TPM3-ALK and TPM4-ALK oncogenes in inflammatory myofibroblastic tumors. *Am J Pathol* 2000;157:377-84.
15. Jazii FR, Najafi Z, Malekzadeh R, Contrads TP, Ziaee AA, Abnet C, et al. Identification of squamous cell carcinoma associated proteins by proteomics and loss of beta tropomyosin expression in esophageal cancer. *World J Gastroenterol* 2006;12:7104-12.
16. Sugawara E, Togashi Y, Kuroda N, Sakata S, Hatano S, Asaka R, et al. Identification of anaplastic lymphoma kinase fusions in renal cancer: large-scale immunohistochemical screening by the intercalated antibody-enhanced polymer method. *Cancer*. 2012 Jan 7. [Epub ahead of print]
17. Soda M, Choi YL, Enomoto M, Takada S, Yamashita Y, Ishikawa S, et al. Identification of the transforming *EML4-ALK* fusion gene in non-small-cell lung cancer. *Nature* 2007;448:561-6.
18. Mosse YP, Laudenslager M, Longo L, Cole KA, Wood A, Attiyeh EF, et al. Identification of ALK as a major familial neuroblastoma predisposition gene. *Nature* 2008;455:930-5.
19. Janoueix-Lerosey I, Lequin D, Brugieres L, Ribeiro A, de Pontual L, Combaret V, et al. Somatic and germline activating mutations of the ALK kinase receptor in neuroblastoma. *Nature* 2008;455:967-70.
20. George RE, Sanda T, Hanna M, Frohling S, Luther W II, Zhang J, et al. Activating mutations in ALK provide a therapeutic target in neuroblastoma. *Nature* 2008;455:975-8.
21. Chen Y, Takita J, Choi YL, Kato M, Ohira M, Sanada M, et al. Oncogenic mutations of ALK kinase in neuroblastoma. *Nature* 2008;455:971-4.
22. Barreca A, Lasorsa E, Riera L, Machiorlatti R, Piva R, Ponzoni M, et al. Anaplastic lymphoma kinase in human cancer. *J Mol Endocrinol* 2011;47:R11-23.
23. Pulford K, Morris SW, Turturro F. Anaplastic lymphoma kinase proteins in growth control and cancer. *J Cell Physiol* 2004;199:330-58.
24. Druker BJ, Talpaz M, Resta DJ, Peng B, Buchdunger E, Ford JM, et al. Efficacy and safety of a specific inhibitor of the BCR-ABL tyrosine kinase in chronic myeloid leukemia. *N Engl J Med* 2001;344:1031-7.
25. Tomlins SA, Rhodes DR, Perner S, Dhanasekaran SM, Mehra R, Sun XW, et al. Recurrent fusion of TMPRSS2 and ETS transcription factor genes in prostate cancer. *Science* 2005;310:644-8.
26. Choi YL, Takeuchi K, Soda M, Inamura K, Togashi Y, Hatano S, et al. Identification of novel isoforms of the *EML4-ALK* transforming gene in non-small cell lung cancer. *Cancer Res* 2008;68:4971-6.
27. Koivunen JP, Mermel C, Zejnullahu K, Murphy C, Lifshits E, Holmes AJ, et al. *EML4-ALK* fusion gene and efficacy of an ALK kinase inhibitor in lung cancer. *Clin Cancer Res* 2008;14:4275-83.
28. Soda M, Takada S, Takeuchi K, Choi YL, Enomoto M, Ueno T, et al. A mouse model for *EML4-ALK*-positive lung cancer. *Proc Natl Acad Sci U S A* 2008;105:19893-7.
29. Chen Z, Sasaki T, Tan X, Carretero J, Shimamura T, Li D, et al. Inhibition of ALK, PI3K/MEK, and HSP90 in murine lung adenocarcinoma induced by *EML4-ALK* fusion oncogene. *Cancer Res* 2010;70:9827-36.
30. Takeuchi K, Choi YL, Soda M, Inamura K, Togashi Y, Hatano S, et al. Multiplex reverse transcription-PCR screening for *EML4-ALK* fusion transcripts. *Clin Cancer Res* 2008;14:6618-24.
31. Wong DW, Leung EL, So KK, Tam IY, Sihoe AD, Cheng LC, et al. The *EML4-ALK* fusion gene is involved in various histologic types of lung cancers from nonsmokers with wild-type EGFR and KRAS. *Cancer* 2009;115:1723-33.
32. Kwak EL, Bang YJ, Camidge DR, Shaw AT, Solomon B, Maki RG, et al. Anaplastic lymphoma kinase inhibition in non-small-cell lung cancer. *N Engl J Med* 2010;363:1693-703.
33. Tiseo M, Gelsomino F, Boggiani D, Bortesi B, Bartolotti M, Bozzetti C, et al. EGFR and *EML4-ALK* gene mutations in NSCLC: a case report of erlotinib-resistant patient with both concomitant mutations. *Lung Cancer* 2011;71:241-3.
34. Takeuchi K, Choi YL, Togashi Y, Soda M, Hatano S, Inamura K, et al. KIF5B-ALK, a novel fusion oncokine identified by an immunohistochemistry-based diagnostic system for ALK-positive lung cancer. *Clin Cancer Res* 2009;15:3143-9.
35. Mino-Kenudson M, Chirieac LR, Law K, Hornick JL, Lindeman N, Mark EJ, et al. A novel, highly sensitive antibody allows for the routine detection of ALK-rearranged lung adenocarcinomas by standard immunohistochemistry. *Clin Cancer Res* 2010;16:1561-71.
36. Yoshida A, Tsuta K, Nakamura H, Kohno T, Takahashi F, Asamura H, et al. Comprehensive histologic analysis of ALK-rearranged lung carcinomas. *Am J Surg Pathol* 2011;35:1226-34.
37. Lin E, Li L, Guan Y, Soriano R, Rivers CS, Mohan S, et al. Exon array profiling detects *EML4-ALK* fusion in breast, colorectal, and non-small cell lung cancers. *Mol Cancer Res* 2009;7:1466-76.
38. Sanders HR, Li HR, Bruey JM, Scheerle JA, Meloni-Ehrig AM, Kelly JC, et al. Exon scanning by reverse transcriptase-polymerase chain reaction for detection of known and novel *EML4-ALK* fusion variants in non-small cell lung cancer. *Cancer Genet* 2011;204:45-52.
39. Christensen JG, Zou HY, Arango ME, Li Q, Lee JH, McDonnell SR, et al. Cytoreductive antitumor activity of PF-2341066, a novel inhibitor of anaplastic lymphoma kinase and c-Met, in experimental models of anaplastic large-cell lymphoma. *Mol Cancer Ther* 2007;6:3314-22.
40. Shaw AT, Yeap BY, Solomon BJ, Riely GJ, Gainor J, Engelman JA, et al. Effect of crizotinib on overall survival in patients with advanced non-small-cell lung cancer harbouring ALK gene rearrangement: a retrospective analysis. *Lancet Oncol* 2011;12:1004-12.
41. Engelman JA, Zejnullahu K, Mitsudomi T, Song Y, Hyland C, Park JO, et al. MET amplification leads to gefitinib resistance in lung cancer by activating ERBB3 signaling. *Science* 2007;316:1039-43.
42. Bergethon K, Shaw AT, Ignatius Ou SH, Katayama R, Lovly CM, McDonald NT, et al. ROS1 rearrangements define a unique molecular class of lung cancers. *J Clin Oncol* 2012;30:863-70.
43. Takeuchi K, Soda M, Togashi Y, Suzuki R, Sakata S, Hatano S, et al. RET, ROS1 and ALK fusions in lung cancer. *Nat Med* 2012;18:378-81.
44. Gerber DE, Minna JD. ALK inhibition for non-small cell lung cancer: from discovery to therapy in record time. *Cancer Cell* 2010;18:548-51.
45. Wong DW, Leung EL, Wong SK, Tin VP, Sihoe AD, Cheng LC, et al. A novel KIF5B-ALK variant in nonsmall cell lung cancer. *Cancer* 2011;117:2709-18.
46. Togashi Y, Soda M, Sakata S, Sugawara E, Hatano S, Asaka R, et al. KLC1-ALK: a novel fusion in lung cancer identified using a formalin-fixed paraffin-embedded tissue only. *PLoS One* 2012;7:e31323.
47. Debelenko LV, Raimondi SC, Daw N, Shivakumar BR, Huang D, Nelson M, et al. Renal cell carcinoma with novel VCL-ALK fusion: new representative of ALK-associated tumor spectrum. *Mod Pathol* 2011;24:430-42.
48. Marino-Enriquez A, Ou WB, Weldon CB, Fletcher JA, Perez-Atayde AR. ALK rearrangement in sickle cell trait-associated renal medullary carcinoma. *Genes Chromosomes Cancer* 2011;50:146-53.
49. Bresler SC, Wood AC, Haglund EA, Courtright J, Belcastro LT, Plegaria JS, et al. Differential inhibitor sensitivity of anaplastic lymphoma kinase variants found in neuroblastoma. *Sci Transl Med* 2011;3:108ra14.
50. Schonherr C, Ruuth K, Yamazaki Y, Eriksson T, Christensen J, Palmer RH, et al. Activating ALK mutations found in neuroblastoma are inhibited by crizotinib and NVP-TAE684. *Biochem J* 2011;440:405-13.
51. Schonherr C, Ruuth K, Eriksson T, Yamazaki Y, Ottmann C, Combaret V, et al. The neuroblastoma ALK(I1250T) mutation is a kinase-dead RTK *in vitro* and *in vivo*. *Transl Oncol* 2011;4:258-65.
52. Murugan AK, Xing M. Anaplastic thyroid cancers harbor novel oncogenic mutations of the ALK gene. *Cancer Res* 2011;71:4403-11.
53. Bagci O, Tumer S, Olgun N, Altungoz O. Copy number status and mutation analyses of anaplastic lymphoma kinase (ALK) gene in 90 sporadic neuroblastoma tumors. *Cancer Lett* 2012;317:72-7.

54. van Gaal JC, Flucke UE, Roeffen MH, de Bont ES, Sleijfer S, Mavinkurve-Groothuis AM, et al. Anaplastic lymphoma kinase aberrations in rhabdomyosarcoma: clinical and prognostic implications. *J Clin Oncol* 2012;30:308–15.
55. Choi YL, Soda M, Yamashita Y, Ueno T, Takashima J, Nakajima T, et al. EML4-ALK mutations in lung cancer that confer resistance to ALK inhibitors. *N Engl J Med* 2010;363:1734–9.
56. Carter TA, Wodicka LM, Shah NP, Velasco AM, Fabian MA, Treiber DK, et al. Inhibition of drug-resistant mutants of ABL, KIT, and EGF receptor kinases. *Proc Natl Acad Sci U S A* 2005;102:11011–6.
57. Sasaki T, Koivunen J, Ogino A, Yanagita M, Niki-forow S, Zheng W, et al. A novel ALK secondary mutation and EGFR signaling cause resistance to ALK kinase inhibitors. *Cancer Res* 2011;71:6051–60.
58. Sasaki T, Okuda K, Zheng W, Butrynski J, Capelletti M, Wang L, et al. The neuroblastoma-associated F1174L ALK mutation causes resistance to an ALK kinase inhibitor in ALK-translocated cancers. *Cancer Res* 2010;70:10038–43.
59. Katayama R, Shaw AT, Khan TM, Mino-Kenudson M, Solomon BJ, Halmos B, et al. Mechanisms of acquired crizotinib resistance in ALK-rearranged lung cancers. *Sci Transl Med* 2012;4:120ra17.
60. Doebele RC, Pilling AB, Aisner DL, Kutateladze TG, Le AT, Weickhardt AJ, et al. Mechanisms of resistance to crizotinib in patients with ALK gene rearranged non-small cell lung cancer. *Clin Cancer Res* 2012;18:1472–82.
61. Katayama R, Khan TM, Benes C, Lifshits E, Ebi H, Rivera VM, et al. Therapeutic strategies to overcome crizotinib resistance in non-small cell lung cancers harboring the fusion oncogene EML4-ALK. *Proc Natl Acad Sci U S A* 2011;108:7535–40.
62. Sakamoto H, Tsukaguchi T, Hiroshima S, Kodama T, Kobayashi T, Fukami TA, et al. CH5424802, a selective ALK inhibitor capable of blocking the resistant gatekeeper mutant. *Cancer Cell* 2011;19:679–90.
63. Butrynski JE, D'Adamo DR, Hornick JL, Dal Cin P, Antonescu CR, Jhanwar SC, et al. Crizotinib in ALK-rearranged inflammatory myofibroblastic tumor. *N Engl J Med* 2010;363:1727–33.
64. Gambacorti-Passerini C, Messa C, Pogliani EM. Crizotinib in anaplastic large-cell lymphoma. *N Engl J Med* 2011;364:775–6.
65. Wellstein A, Toretzky JA. Hunting ALK to feed targeted cancer therapy. *Nat Med* 2011;17:290–1.
66. Vardiman JW, Thiele J, Arber DA, Brunning RD, Borowitz MJ, Porwit A, et al. The 2008 revision of the World Health Organization (WHO) classification of myeloid neoplasms and acute leukemia: rationale and important changes. *Blood* 2009;114:937–51.
67. Mok TS, Wu YL, Thongprasert S, Yang CH, Chu DT, Saijo N, et al. Gefitinib or carboplatin-paclitaxel in pulmonary adenocarcinoma. *N Engl J Med* 2009;361:947–57.
68. Zou HY, Li Q, Lee JH, Arango ME, McDonnell SR, Yamazaki S, et al. An orally available small-molecule inhibitor of c-Met, PF-2341066, exhibits cytoreductive antitumor efficacy through antiproliferative and antiangiogenic mechanisms. *Cancer Res* 2007;67:4408–17.



ALK fusion gene positive lung cancer and 3 cases treated with an inhibitor for ALK kinase activity

Hideki Kimura^{a,*}, Takahiro Nakajima^{a,d}, Kengo Takeuchi^b, Manabu Soda^c, Hiroyuki Mano^c, Toshihiko Iizasa^a, Yukiko Matsui^a, Mitsuru Yoshino^a, Masato Shingyoji^a, Meiji Itakura^a, Makiko Itami^e, Dai Ikebe^e, Sana Yokoi^f, Hajime Kageyama^f, Miki Ohira^g, Akira Nakagawara^h

^a Division of Thoracic Diseases, Chiba Cancer Center, Chiba, Japan

^b Pathology Project for Molecular Targets, Cancer Institute, Japanese Foundation for Cancer Research (JFCR), Koto, Tokyo, Japan

^c Division of Functional Genomics, Jichi Medical University, Tochigi, Japan

^d Division of Thoracic Surgery, Toronto General Hospital, University Health Network, Toronto, Canada

^e Division of Pathology, Chiba Cancer Center, Japan

^f Cancer Genome Center, Chiba Cancer Center Research Institute, Japan

^g Laboratory of Cancer Genomics, Chiba Cancer Center Research Institute, Japan

^h Chiba Cancer Center, Japan

ARTICLE INFO

Article history:

Received 16 October 2010

Received in revised form 24 May 2011

Accepted 30 May 2011

Key words:

ALK
EML4
KIF5B
Fusion gene
Lung cancer
EBUS
TBNA
Crizotinib
ALK inhibitor

ABSTRACT

Background: Anaplastic lymphoma kinase (ALK) fusion gene-positive lung cancer accounts for 4–5% of non-small cell lung carcinoma. A clinical trial of the specific inhibitor of ALK fusion-type tyrosine kinase is currently under way.

Methods: ALK fusion gene products were analyzed immunohistochemically with the materials obtained by surgery or by endobronchial ultrasound-guided transbronchial needle aspiration (EBUS-TBNA). The echinoderm microtubule-associated protein-like 4 (EML4)-ALK or kinesin family member 5B (KIF5B)-ALK translocation was confirmed by the reverse transcription polymerase chain reaction (RT-PCR) and fluorescence in situ hybridization (FISH). After eligibility criteria were met and informed consent was obtained, 3 patients were enrolled for the Pfizer Study of Crizotinib (PF02341066), Clinical Trial A8081001, conducted at Seoul National University.

Results: Out of 404 cases, there were 14 of EML4-ALK non-small cell carcinoma (NSCLC) and one KIF5B-ALK NSCLC case (8 men, 7 women; mean age, 61.9 years, range 48–82). Except for 2 light smokers, all patients were non-smokers. All cases were of adenocarcinoma with papillary or acinar subtypes. Three were of stage IA, 5 of stage IIIA, 1 of stage IIIB and 6 of stage IV. Ten patients underwent thoracotomy, 3 received chemotherapy and 2 only best supportive care (BSC). One BSC and 2 chemotherapy cases were enrolled for the clinical trial. Patients with advanced stages who received chemotherapy or best supportive care were younger (54.0 ± 6.3) than those who were surgically treated (65.8 ± 10.1) ($p < 0.05$).

The powerful effect of ALK inhibitor on EML4-ALK NSCLC was observed. Soon after its administration, almost all the multiple bone and lymph node metastases quickly disappeared. Nausea, diarrhea and the persistence of a light image were the main side effects, but they diminished within a few months.

Conclusion: ALK-fusion gene was found in 3.7% (15/404) NSCLC cases and advanced disease with this fusion gene was correlated with younger generation. The ALK inhibitor presented in this study is effective in EML4-ALK NSCLC cases. A further study will be necessary to evaluate the clinical effectiveness of this drug.

© 2011 Elsevier Ireland Ltd. All rights reserved.

1. Introduction

As the mechanisms of carcinogenesis become clearer, the target of cancer treatment is shifting from non-specific cytotoxic agents to specific agents that block key molecular events in the carcinogenesis of malignancy such as EGFR-TKI and anti-HER2 antibody (trastuzumab) [1–3]. Recently, Mano et al. [4–6] reported that a small inversion within chromosome 2p results in the formation of a fusion gene comprising portions of the

* Corresponding author at: Division of Thoracic Diseases, Chiba Cancer Center, 666-2, Nitona-cho, Chuo-ku, 260-8717 Chiba, Japan. Tel.: +81 43 264 5431; fax: +81 43 262 8680.

E-mail address: hkimura@chiba-cc.jp (H. Kimura).

echinoderm microtubule-associated protein-like 4 (EML4) gene and the anaplastic lymphoma kinase (ALK) gene in non-small-cell lung cancer. Transgenic mice that express EML4-ALK specifically in lung epithelial cells develop multiple foci of adenocarcinoma in the lung soon after birth, and the oral administration of a specific inhibitor of ALK tyrosine kinase activity eradicated completely the foci of adenocarcinoma. Clinical trials of specific inhibitors of EML4-ALK tumors are currently underway [7–11]. Kwak et al. [11] reported the effect of crizotinib in Clinical Trial A8081001 on the 82 patients with advanced ALK-positive disease. Over a mean treatment duration of 6.4 months, the overall response rate was 57% and the estimated probability of 6-month progression-free survival was 72%. We report 15 cases of ALK fusion gene-positive NSCLC cases and 3 cases in our experience with ALK inhibitor in the Pfizer Study of crizotinib (PF02341066), Clinical Trial A8081001, which was conducted at Seoul National University.

2. Materials and methods

Out of 404 patients who had undergone surgical resection (295 cases) or bronchoscopy (109 cases) in Chiba Cancer Center, Japan, from 2007 to 2009, 15 ALK fusion gene-positive NSCLC patients were initially screened by immunohistochemical procedures. Diagnoses were confirmed by RT-PCR and/or FISH for their molecular translocation.

2.1. ALK fusion protein detection by immunohistochemical methods

The intercalated antibody-enhanced polymer method of Takeuchi et al. [12,13] was used to detect ALK proteins. Formalin-fixed paraffin-embedded tissue was sliced at a thickness of 4 μm and the sections were placed on silane-coated slides. For antigen retrieval, the slides were heated for 40 min at 97 °C in target Retrieval Solution (pH 9.0; Dako). They were then incubated at room temperature, first with Protein Block Serum-free Ready-to-Use solution (Dako) for 10 min, and then with an anti-ALK antibody (5A4, Abcam) for 30 min. To increase the sensitivity of detection, we included an incubation step of 15 min at room temperature with rabbit polyclonal antibodies to mouse immunoglobulin (Dako). The immune complexes were then detected with the dextran polymer reagent and an AutoStainer instrument (Dako).

2.2. Confirmation of EML4-ALK fusion gene by RT-PCR and FISH

We confirmed the existence of ALK fusion gene expression by fluorescence in situ hybridization (FISH) and/or by the reverse transcription-polymerase chain reaction (RT-PCR).

2.3. Fluorescence in situ hybridization (FISH)

An EML4-ALK fusion assay was performed [10–12]. Unstained sections were processed with a Histology FISH Accessory Kit (Dako), subjected to hybridization with fluorescence-labeled bacterial artificial chromosome clone probes for EML4 and ALK (self-produced probes; EML4: RP11-996L7, ALK: RP11-984I21 and RP11-62B19), stained with 4,6-diamidino-2-phenylindole, and examined with a fluorescence microscope (BX51; Olympus). The FISH positivity criteria specified “over 50% cancer cells” for EBUS-TBNA samples.

2.4. Reverse transcription-polymerase chain reaction (RT-PCR)

The multiplex PCR method proposed by the Japanese ALK lung cancer study group (ALCAS) was used to confirm the expression of ALK fusion gene [4–6].

Table 1
Characteristics of ALK fusion gene positive lung cancer patients.

Patient no	Sex	Age	SI	Variant	p Stage	Therapy	Recurrence	Distant meta	Survival (M)	Prognosis	ALK inhibitor case no
1	f	64	0	3	IIIA	Surgery	Positive	Bone, brain	21	Dead	
2	m	82	0	2	IIIA	Surgery	Positive	Ascites	36	Alive	
3	f	68	0	3	IIIB	Surgery	Positive	Brain	34	Alive	
4	f	60	0	3	IIIA	Surgery	Negative	None	29	Alive	
5	m	73	0	3	IA	Surgery	Negative	None	21	Alive	
6	m	66	0	KIF5B	IA	Surgery	Negative	None	15	Alive	
7	m	56	300	1	IA	Surgery	Negative	None	13	Alive	
8	m	46	0	5	IIIA	Surgery	Negative	None	22	Alive	
9	m	71	0	1	IIIA	Surgery	Negative	None	17	Alive	
10	f	73	0	1	IV	Surgery	Negative	None	14	Alive	
11	m	55	100	3	IV	BSC		Bone, brain	5	Dead	
12	m	48	0	1	IV	Chemo		Bone, brain	29	Dead	Case 1
13	f	49	0	3	IV	BSC		Bone, brain	15	Alive	Case 2
14	f	54	0	1	IV	Chemo		Bone, brain, pul	22	Alive	Case 3
15	f	64	0	3	IV	Chemo		Pul	2	Alive	

SI, smoking index; f, female; m, male; Ad, adenocarcinoma; muc+, mucin production; Distant meta, at the recurrence (surgery group); pul, pulmonary metastasis; Case 1 was already reported by Nakajima et al. [16].

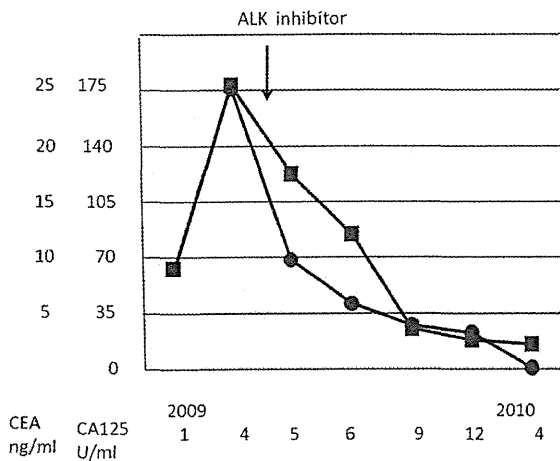


Fig. 1. Changes of tumor markers before and during the treatment with ALK inhibitor (Case 1) CEA (■), CA125 (●). Marked reduction of tumor markers was observed.

Total RNA was isolated from EBUS-TBNA or surgical samples using AllPrep DNA/RNA Mini Kit (Qiagen) and was reverse-transcribed into single strand cDNA using a High Capacity RNA-to-cDNA Kit (Applied Biosystems). To detect a fusion cDNA derived from EML4 or KIF5B and ALK, PCR analysis was performed with the AmpliTaq Gold PCR Master Mix (Applied Biosystems), the forward primers derived from EML4, EA-F-cDNA-S (5'-GTGCAGTGTITAGCATTCTTGGG-3'), EA-F-2-g-S (5'-AGCTACATCACACACCTTGACTGG-3'), EA-F-cDNA-v3-S-2 (5'-TACCAGTGCTGTCTCAATTGCAGG-3'') and EA-W-cDNA-in-S (5'-GCTTCCCGCAAGATGGACGG-3') and the forward primers derived from KIF5B, KA-F-cDNA-S-e24 (5'-CAGCTGAGAGAGTCAAAGCTTTGG-3'), KA-F-cDNA-S-e17 (5'-GACAGTTGGAGGAATCTGTCGATG-3'), KA-F-cDNA-S-e11

B

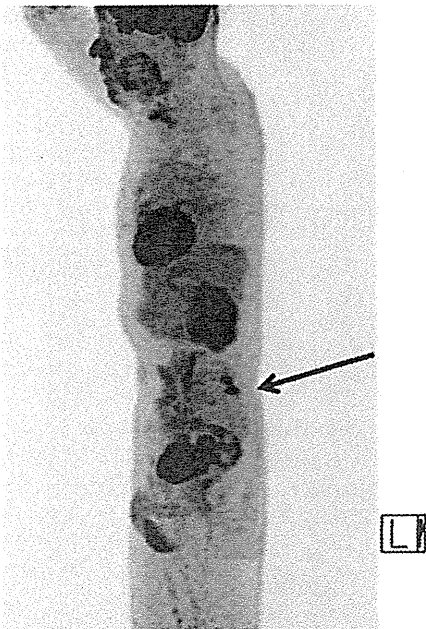


Fig. 2. FDG-PET scan of Case 1 performed at the same time (09/28/2009) as the previously reported Fig. 1D (Nakajima et al. [16]) shows bone metastasis of the left vertebral arch of L5 (arrow) in a sagittal view.

(5'-ATCCTGCGGAACACTATTTCAGTGG-3'), and KA-cDNA-S-e2 (5'-TCAAGCACATCTCAAGAGCAAGTG-3') and the reverse primer derived from ALK, EA-F-cDNA-A (5'-TCTTGCCAGCAAAG-CAGTAGTTGG-3'). PCR products were purified from gel bands using QIAquick Gel Extraction Kit (Qiagen) and confirmed by direct sequencing analysis.

2.5. Enrolment of patients for the Clinical Trial A8081001

Informed consent was obtained from each patient to be enrolled for the study [10]. Eligibility criteria for the enrolment of ALK translocation positive patients into the ALK TKI PI Trial were as required by the Committee of Clinical Trials A8081001.

3. Results

There were 15 ALK fusion gene-positive cases which were screened immunohistochemically and confirmed by RT-PCR and FISH [14,15]. Eight patients were men and 7 women, of mean age

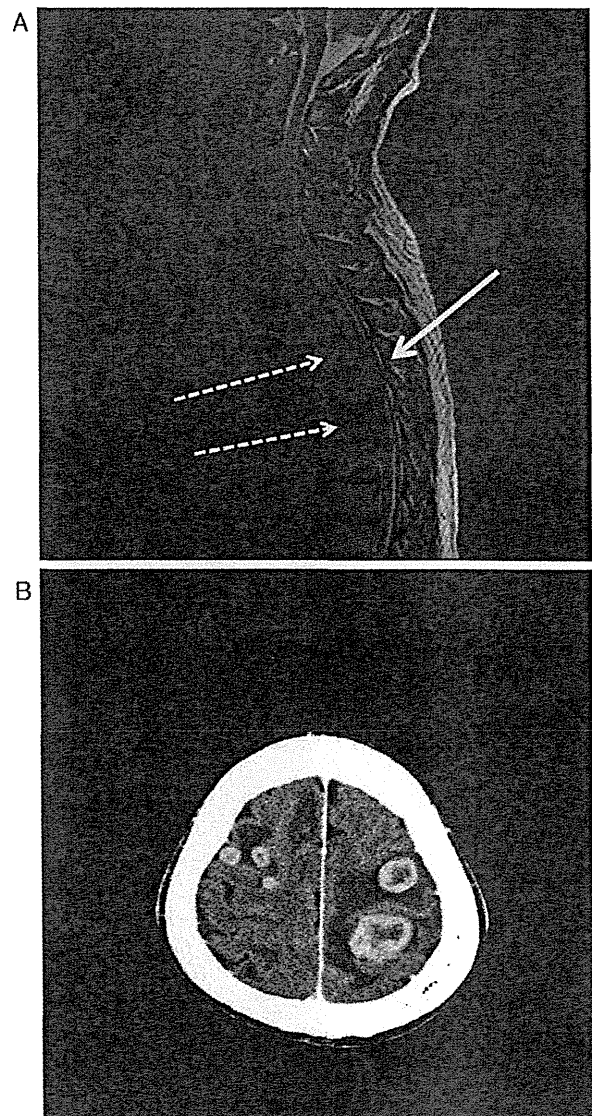


Fig. 3. MRI (Case 1) of the spinal cord on 04/05/2010 shows the metastases to the spinal cord (straight allow) and the spinal column (Th 4,6 dotted allow). B. CT scan (Case 1) of the brain on 04/05/2010 shows multiple brain metastases.

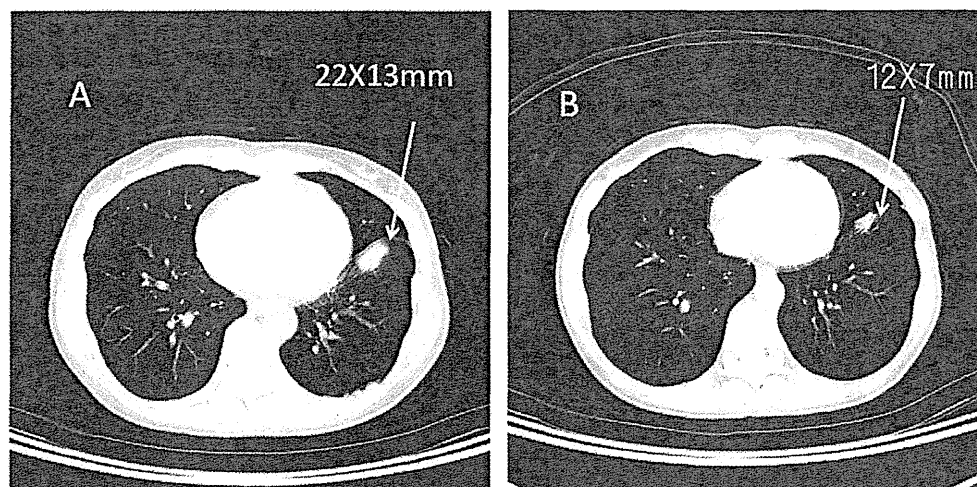


Fig. 4. CT scan (Case 2): A, 07/22/2009 (before ALK inhibitor) and B, 09/02/2009 (5 weeks after the initiation of the therapy). Left S8 tumor (arrow) decreased in size from 22X13 mm to 12X7 mm (PR).

61.9 years (range 48–82). Most were non-smokers, but 2 smoked lightly (Table 1). All tumors were adenocarcinomas with a papillary pattern predominant (5 cases), an acinar pattern predominant (3 cases), with mucin production (4 cases), etc. There were fourteen cases of fusion with EML4 and one KIF5B gene. There were 7 variant 3, 5 variant 1, and 1 each of variants 2 and 5. There were 3 stage IA, 5 stage IIIA, 1 stage IIIB and 6 stage IV cases. Ten cases were diagnosed after surgical resection, and 5, by tissue samples obtained with EBUS-TBNA. Ten cases underwent thoracotomy, 3 cases, chemotherapy, and 2 cases, only best supportive care. Of 5 cases diagnosed by EBUS-TBNA, 2 cases receiving chemotherapy and one receiving best supportive care were enrolled for the clinical trial. The mean age of the surgically treated group was 65.8 ± 10.1 ,

and that of chemotherapy and BSC group was 54.0 ± 6.3 . The difference was found by Student's *t* test to be statistically significant ($p < 0.05$), indicating that younger patients tend to have advanced cancer.

Out of 10 surgically treated cases, seven survived without a sign of recurrence, 3 had recurrence in both bone and brain tissue, and one died of bone and lymph node metastasis.

3.1. Case 1

Case 1 has already been reported in a case report (Nakajima et al.) [16] but without precise descriptions of the response to crizotinib, the adverse effects, the pattern of recurrence or the metastatic

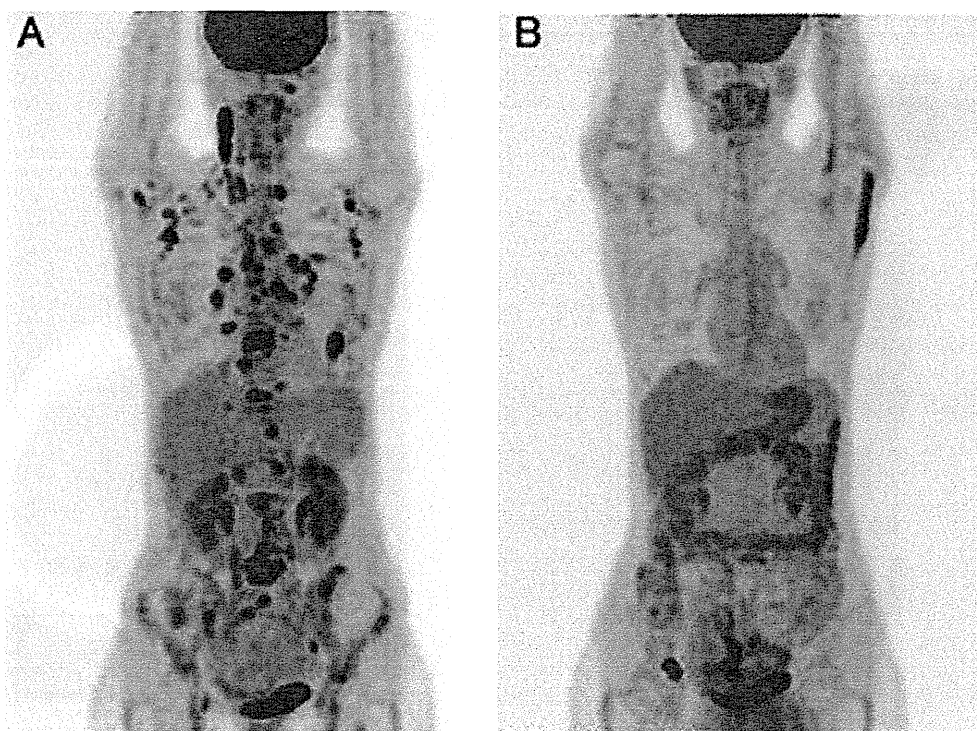


Fig. 5. FDG-PET scan (Case 2): A, 07/22/2009 (before ALK inhibitor) and B, 03/10/2010 FDG-PET scan shows marked reduction of accumulation in multiple bone and lymph node metastases 7 months after the initiation of the treatment.

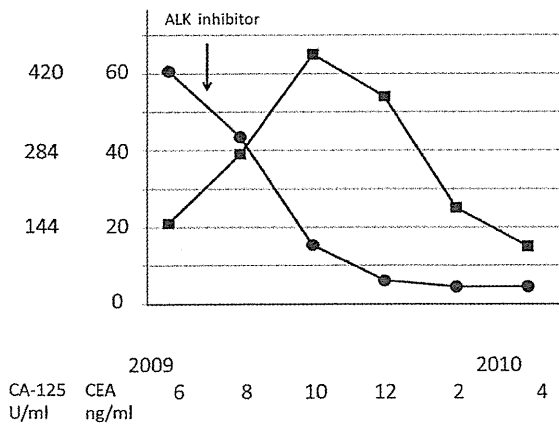


Fig. 6. Changes of tumor markers before and during the treatment with ALK inhibitor in case 2. CA125 (●) gradually decreased along with the treatment, but CEA (■) increased soon after the initiation of the therapy. The value of CEA then gradually decreased to 15.2 ng/ml in April 2010 (after 10 months).

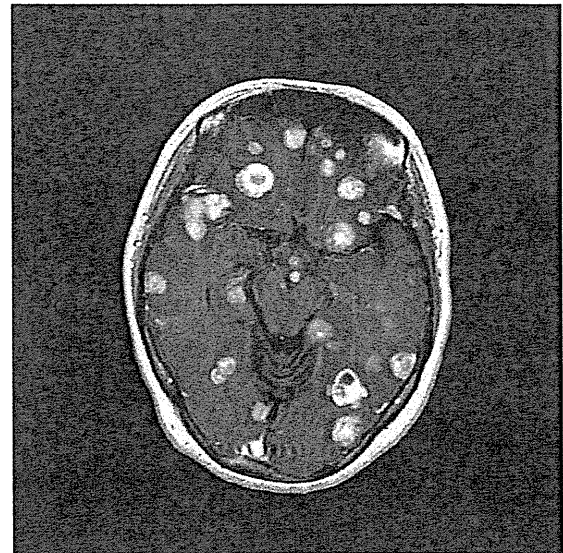


Fig. 7. Brain MRI of case 2 on 7/30/2010 showing multiple metastases.

tumor lesions. Such descriptions may contribute to a better understanding of the other cases, and so case 1 is described briefly below.

A 48-year-old non-smoking male patient had lung adenocarcinoma in the right lower lobe and multiple bone and lymph node metastases (T3N2M1 stage IV) at his first medical examination in November 2007. After several courses of chemotherapy, the patient was enrolled in a trial of crizotinib (PF02341066) from May 5th 2009 at Seoul National University, in which the drug was orally administered at 500 mg/day.

The effect of ALK inhibitor appeared rapidly. The patient's dyspnea improved within one week after drug administration. PS improved from 2 to 0 and a marked reduction in the tumor markers was observed (Fig. 1). Within 3 months after the start of therapy, almost all metastases disappeared except for those at the left vertebral arch of L5 (Fig. 2, arrow). The patient had severe adverse effects:

diarrhea, nausea and persistence of light images started soon after the administration of the drug, but these gradually diminished over a 3-week period.

The control of the primary and metastatic tumors continued for 11 months until the patient visited Seoul University in April 2010, when he was hospitalized for paralysis of the lower extremities. MRI revealed spinal column (Th4-6) and spinal cord metastases (Fig. 3A). Soon after his hospitalization in our Cancer Center in April 2010, multiple brain metastases (Fig. 3B) were found, so the drug administration was stopped and he was transferred to a palliative care unit.

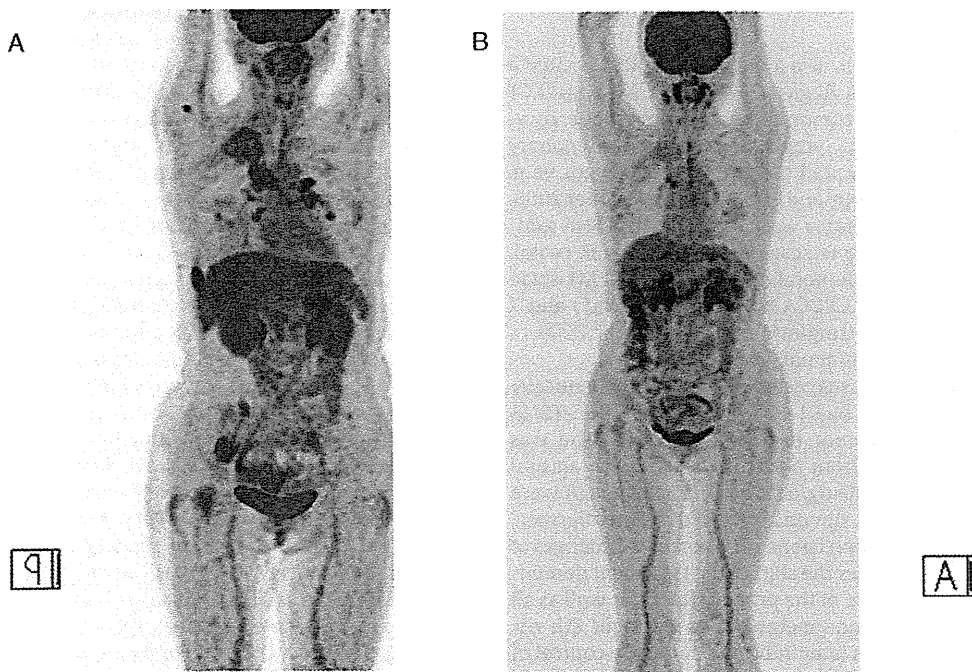


Fig. 8. FDG-PET scan: A, 09/08/2009 (before ALK inhibitor) and B, 07/05/2010 FDG-PET scan follow-up for 10 months indicated complete control of primary and distant metastases in case 3.

3.2. Case 2

A 49-year-old woman, a non-smoker with no history of illness, PS0, was introduced to the Orthopedics Department of our Center in April 2009 for back pain and multiple osteoplastic changes in the bones. Systematic examination revealed an abnormal shadow 22X13 mm in size in the left lower lobe (Fig. 4A). Bronchoscopy and a PET scan indicated left S8 adenocarcinoma with cervical, axial, mediastinal, hilar, pancreatic and retroperitoneal lymph node metastases, as well as cranial, thoracic (Th1–12), lumbar (L1–5), rib (1–12) pelvis, humerus, and femur metastases (Fig. 5A).

She refused any therapy except for best supportive care. One month after the examination, an additional immunohistochemical examination for EML4-ALK fusion protein was performed, and found to be positive. The presence of mRNA for EML4-ALK gene was also confirmed by RT-PCR and FISH from the mediastinal #4R lymph nodes obtained with EBUS-TBNA, which was performed 2 months later. EGFR mutation was negative, but the direct sequence of the EML4-ALK mRNA indicated that the translocation was variant 3 [9]. She decided to be enrolled to the crizotinib study (PF02341066) at a dosage of 500 mg/day at Seoul National University from July 2009.

She had nausea, diarrhea and light image persistence as in case 1, but her gastrointestinal symptoms were severer than those in case 1. Two weeks after the administration of ALK inhibitor, her back pain disappeared. A PET scan performed 5 weeks after the initiation of the therapy showed marked reduction of bone and lymph node metastases, and the primary tumor had decreased in size from 22X13 mm to 12X7 mm (Fig. 4A and B). Also, the SUV max dropped from 10.7 to 2.42. Changes of tumor markers were not parallel with the clinical course since the measured value of CA-125 dropped from 424 to 107 U/ml, but that of CEA increased from 21.5 to 65.4 ng/ml 4 months later. The value of CEA then gradually decreased to 15.2 ng/ml in April 2010 (10 months after that: Fig. 6). The PET scan conducted after 7 months indicated a partial response to multiple bone and lymph node metastases (Fig. 5B). The patient continued to take the drug until the end of July 2010, when brain metastases (Fig. 7) were found.

3.3. Case 3

A fifty-four-year-old woman, also a non-smoker, PS0, visited a doctor because of back pain in August 2008. Chest X-ray and CT scan showed an S3 59X22 mm tumor in the right upper lobe, combined with #4R, #2R mediastinal lymph nodes and intrapulmonary metastases. The tumor had invaded the SVC and the azygos vein. She had undergone bronchoscopy and EBUS-TBNA in October 2008. A diagnosis of lung adenocarcinoma was obtained with TBNA samples from #7 lymph nodes. Bone scans indicated cranial, costal, vertebral, scapular, pelvic and femoral metastases (T4N2M1 stage IV). She received 2 courses of CBDCA+GEM (1000 mg/m²) and 7 courses of docetaxel (TXTL: 60 mg/m²) from November 2008 to June 2009, but the effect was minimal.

EML4-ALK fusion gene was suggested immunohistochemically in August 2009 and confirmed by RT-PCR obtained by EBUS-TBNA samples from the primary tumor in September 2009. She was enrolled for the clinical trial from November 2009 with an oral administration of crizotinib 500 mg/day. Dyspnea and cough were alleviated within 2 weeks, and she complained of severe diarrhea, nausea, vomiting, light image persistence and perceived changes of taste. A PET scan one month after the start of the treatment demonstrated complete disappearance of the primary tumor as well as all the metastases except for a bone metastasis to the right 8th rib. A PET scan follow-up 8 months later indicated complete control of primary and metastatic tumors (Fig. 8A and B). CEA declined slowly from 1764 ng/ml to 79 ng/ml 6 months after the start of administration (Fig. 9). The patient had 12 brain metastases from 5 mm³

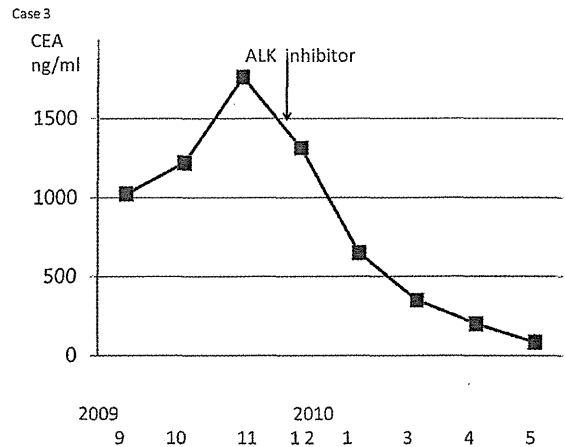


Fig. 9. CEA (■) declined slowly from 1764 ng/ml to 79 ng/ml 6 months after the start of the therapy in case 3.

to 309 mm³ in volume and underwent gamma knife irradiation in August 2009, 2 months before the start of ALK inhibitor treatment. The irradiated field still showed little change for 5 months, but small new lesions appeared in the left occipital area 6 months after the start of the trial. Brain metastases grew very slowly, so we have maintained our observation until October 2010.

4. Discussion

Above, we have reported the far-reaching effects of an ALK inhibitor on EML4-ALK-positive lung cancer patients. Soon after the administration of crizotinib, almost all metastases to bone and lymph nodes rapidly disappeared, followed by a marked reduction in the level of tumor markers in the sera. These observations clearly support the pivotal role of EML4-ALK oncokininase for the growth/survival of not only primary tumors but of the metastases. Such profound effects were rare among the patients when treated with conventional cytotoxic anticancer drugs.

The three cases which were enrolled for the study had surprisingly similar biological characteristics. They had multiple bone and lymph node metastases at the first medical examination, and were non-smokers at younger ages (48–54) who were resistant to chemotherapy. Adverse effects with crizotinib were also similar among them, including transient diarrhea, nausea, light image persistence, and subjective changes of taste. In addition, their response to ALK inhibitor was similar. Bone and lymph node metastases had disappeared within one month after the initiation of the therapy. The response of the primary tumor in case 2 was relatively slow compared with those of the metastases. The difference between the response of primary tumor and metastases to the ALK inhibitor in this case seems to indicate that the similar subclones of tumor cells in the primary tumors that were highly responsive to ALK inhibitor metastasized to distant organs and may give some explanation for the discrepancy in the time-course between CEA and CA125.

Molecular and immunohistochemical analyses in this cohort were conducted on the basis of the specimens obtained through EBUS-TBNA. Originally, EBUS-TBNA had been proposed useful for the pathological diagnosis of mediastinal involvement (N2 disease) of lung cancer [17–20]. However, we have already reported that EBUS-TBNA is also a versatile way of obtaining histological samples for the molecular analyses of cancer-related genes, such as EGFR, p53 et al. [21,22]. For those who have advanced NSCLC, it is often difficult to conduct surgery to obtain specimens from patients. Among such cases, however, EBUS-TBNA can usually be safely carried out to obtain specimens from enlarged mediastinal

lymph nodes or paratracheal tumors. We carried out EBUS-TBNA procedure for the reasons of its advantage in obtaining high quality core samples adequate for this purpose as well as its safety. We do not disregard the importance of TBB for the diagnosis of lung cancer; however, we needed histological samples to examine the immunohistochemistry and FISH for enrolment in a trial of crizotinib. Our experience with the three cases clearly demonstrates the importance and clinical relevance of obtaining such specimens for molecular analyses.

Although the initial effects of crizotinib are substantial in our cases, as well as in those reported by Bang et al. [10,11], such efficacy may not always last long. There was, for instance, development (case 1 and 2) and recurrence (case 3) of brain metastases while favorable control was maintained outside the brain. Given that the primary tumors and lymph node metastases were under control of crizotinib even at the appearance of brain metastases, the tumor cells outside the brain did not lose sensitivity to crizotinib. Relapses in the brain only may indicate either (i) subclones of the tumor acquired both the homing ability to the brain and resistance to crizotinib, or (ii) crizotinib may not penetrate the blood-brain barrier, leading to insufficient concentrations of crizotinib in the brain. It is thus highly important to examine in detail the molecular basis that would account for such acquired resistance to crizotinib, which may be secondary mutations within EML4-ALK itself or mutations/gene amplification of other genes, as demonstrated in the cases of acquired resistance of NSCLC to gefitinib/erlotinib [23–26].

Conflict of interest

None declared.

Acknowledgements

We are grateful to Dr. Yung-Jue Bang and the medical staff of Seoul National University Hospital for their support in the treatment of these patients. We also thank Mr. C.W.P. Reynolds of the Department of International Medical Communications, Tokyo Medical University, for his careful revision of the English of this manuscript.

References

- [1] Janku F, Stewart DJ, Kurzrock R. Targeted therapy in non-small-cell lung cancer—Is it becoming a reality? *Nat Rev Clin Oncol* 2010 Jun 15;7(July (7)):401–14.
- [2] Heinrich MC, Owzar K, Corless CL, et al. Correlation of kinase genotype and clinical outcome in the North American intergroup phase III trial of imatinib mesylate for treatment of advanced gastrointestinal stromal tumor: CALGB 150105 study by cancer and leukemia group B and southwest oncology group. *J Clin Oncol* 2008;26:5360–7.
- [3] Mok TS, Wu YL, Yu CJ, et al. Randomized, placebo-controlled, phase II study of sequential erlotinib and chemotherapy as first-line treatment for advanced non-small-cell lung cancer. *J Clin Oncol* 2009;27:5080–7.
- [4] Soda M, Choi YL, Enomoto M, et al. Identification of the transforming EML4-ALK fusion gene in non-small-cell lung cancer. *Nature* 2007;448:561–6.
- [5] Mano H. Non-solid oncogenes in solid tumors: EML4-ALK fusion genes in lung cancer. *Cancer Sci* 2008;99:2349–55.
- [6] Soda M, Takada S, Takeuchi K, et al. A mouse model for EML4-ALK-positive lung cancer. *Proc Natl Acad Sci USA* 2008;105:19893–7.
- [7] Christensen JG, Zou HY, Arango ME, et al. Cyto-reductive antitumor activity of PF-2341066, a novel inhibitor of anaplastic lymphoma kinase and c-Met, in experimental models of anaplastic large-cell lymphoma. *Mol Cancer Ther* 2007;6:3314–22.
- [8] Koivunen JP, Mermel C, Zejnullahu K, et al. EML4-ALK fusion gene and efficacy of an ALK kinase inhibitor in lung cancer. *Clin Cancer Res* 2008;14:4275–83.
- [9] Kwak EL, Camidge DR, Clark J, et al. Clinical activity observed in a phase I dose escalation trial of an oral c-met and ALK inhibitor, PF-02341066. *J Clin Oncol* 2009;27:155.
- [10] Bang Y, Kwak EL, Shaw AT, et al. Clinical activity of the oral ALK inhibitor PF-02341066 in ALK-positive patients with non-small cell lung cancer (NSCLC). *J Clin Oncol* 2010;28:18s [suppl]; abstr 3].
- [11] Kwak EL, Bang YJ, Camidge DR, et al. Anaplastic lymphoma kinase inhibition in non-small-cell lung cancer. *N Engl J Med* 2010;363:1693–703.
- [12] Takeuchi K, Choi YL, Togashi Y, et al. KIF5B-ALK, a novel fusion oncogene identified by an immunohistochemistry-based diagnostic system for ALK-positive lung cancer. *Clin Cancer Res* 2009;15:3143–9.
- [13] Inamura K, Takeuchi K, Togashi Y, et al. EML4-ALK lung cancers are characterized by rare other mutations, a TTF-1 cell lineage, an acinar histology, and young onset. *Mod Pathol* 2009;22:508–15.
- [14] Shaw AT, Yeap BY, Mino-Kenudson M, et al. Clinical features and outcome of patients with non-small-cell lung cancer who harbor EML4-ALK. *J Clin Oncol* 2009;27(September (26)):4247–53.
- [15] Takahashi T, Snooze M, Kobayashi M, et al. Clinicopathologic features of non-small-cell lung cancer with EML4-ALK fusion gene. *Ann Surg Oncol* 2010;17(March (3)):889–97.
- [16] Nakajima T, Kimura H, Takeuchi K, et al. Treatment of lung cancer with an ALK inhibitor after EML4-ALK fusion gene detection using endobronchial ultrasound-guided transbronchial needle aspiration. *J Thorac Oncol* 2010;5:2041–3.
- [17] Yasufuku K, Chiyo M, Koh E, et al. Endobronchial ultrasound guided transbronchial needle aspiration for staging of lung cancer. *Lung Cancer* 2005;50:347–54.
- [18] Yasufuku K, Chiyo M, Sekine Y, et al. Real-time endobronchial ultrasound-guided transbronchial needle aspiration of mediastinal and hilar lymph nodes. *Chest* 2004;126:122–8.
- [19] Herth FJ, Eberhardt R, Vilmann P, Krasnik M, Ernst A. Real-time endobronchial ultrasound guided transbronchial needle aspiration for sampling mediastinal lymph nodes. *Thorax* 2006;61:795–8.
- [20] Herth FJ, Ernst A, Eberhardt R, Vilmann P, Dienemann H, Krasnik M. Endobronchial ultrasound-guided transbronchial needle aspiration of lymph nodes in the radiologically normal mediastinum. *Eur Respir J* 2006;28:910–4.
- [21] Nakajima T, Yasufuku K, Suzuki M, et al. Assessment of epidermal growth factor receptor mutation by endobronchial ultrasound-guided transbronchial needle aspiration. *Chest* 2007;132:597–602.
- [22] Mohamed S, Yasufuku K, Nakajima T, et al. Analysis of cell cycle-related proteins in mediastinal lymph nodes of patients with N2-NSCLC obtained by EBUS-TBNA: relevance to chemotherapy response. *Thorax* 2008;63:642–7.
- [23] Kobayashi S, Boggon TJ, Dayaram T, et al. EGFR mutation and resistance of non-small-cell lung cancer to gefitinib. *N Engl J Med* 2005;352:786–92.
- [24] Lu L, Ghose AK, Quail MR, et al. ALK mutants in the kinase domain exhibit altered kinase activity and differential sensitivity to small molecule ALK inhibitors. *Biochemistry* 2009;48:3600–9.
- [25] Gazdar AF. Activating and resistance mutations of EGFR in non-small-cell lung cancer: role in clinical response to EGFR tyrosine kinase inhibitors. *Oncogene* 2009;28:S24–31.
- [26] Choi YL, Soda M, Yamashita Y, et al. EML4-ALK mutations in lung cancer that confer resistance to ALK inhibitors. *N Engl J Med* 2010;363:1734–9.

Oncogenic *MAP2K1* mutations in human epithelial tumorsYoung Lim Choi^{1,2}, Manabu Soda¹, Toshihide Ueno¹, Toru Hamada¹, Hidenori Haruta¹, Azusa Yamato¹, Kazutaka Fukumura², Mizuo Ando², Masahito Kawazu², Yoshihiro Yamashita¹ and Hiroyuki Mano^{1,2,3,*}¹Division of Functional Genomics, Jichi Medical University, Tochigi 329-0498, Japan, ²Department of Medical Genomics, Graduate School of Medicine, University of Tokyo, Tokyo 113-0033, Japan and ³Core Research for Evolutional Science and Technology, Japan Science and Technology Agency, Saitama 332-0012, Japan*To whom correspondence should be addressed. Tel: +81 285 58 7449;
Fax: +81 285 44 7322;
Email: hmano@jichi.ac.jp

The scirrhous subtype of gastric cancer is a highly infiltrative tumor with a poor outcome. To identify a transforming gene in this intractable disorder, we constructed a retroviral complementary DNA (cDNA) expression library from a cell line (OCUM-1) of scirrhous gastric cancer. A focus formation assay with the library and mouse 3T3 fibroblasts led to the discovery of a transforming cDNA, encoding for MAP2K1 with a glutamine-to-proline substitution at amino acid position 56. Interestingly, treatment with a MAP2K1-specific inhibitor clearly induced cell death of OCUM-1 but not of other two cell lines of scirrhous gastric cancer that do not carry MAP2K1 mutations, revealing the essential role of MAP2K1(Q56P) in the transformation mechanism of OCUM-1 cells. By using a next-generation sequencer, we further conducted deep sequencing of the *MAP2K1* cDNA among 171 human cancer specimens or cell lines, resulting in the identification of one known (D67N) and four novel (R47Q, R49L, I204T and P306H) mutations within MAP2K1. The latter four changes were further shown to confer transforming potential to MAP2K1. In our experiments, a total of six (3.5%) activating mutations in MAP2K1 were thus identified among 172 of specimens or cell lines for human epithelial tumors. Given the addiction of cancer cells to the elevated MAP2K1 activity for proliferation, human cancers with such MAP2K1 mutations are suitable targets for the treatment with MAP2K1 inhibitors.

Introduction

Many growth-promoting or survival signals converge on members of the RAS family of small guanosine triphosphatases, which then activate the mitogen-activated protein kinase (MAPK) signaling pathway, eventually leading to the transcriptional activation or repression of specific genes in the nucleus (1,2). In addition to such canonical RAS-MAPK signaling, RAS-mediated signaling engages in cross talk with various other signaling pathways, such as those mediated by phosphoinositide 3-kinase (3), Janus kinases (4) as well as WNT and β -catenin (5).

Reflecting the central role of the RAS-MAPK cascade in cell proliferation, activated mutants of RAS family members (HRAS, KRAS and NRAS) are among the oncoproteins most frequently detected in human malignancies (2). Discovery of mutations of BRAF in melanoma and colorectal carcinoma further reinforces the substantial contribution of the RAS-MAPK cascade to carcinogenesis (6). The contributions of somatic mutations of other participants in the RAS-MAPK cascade to human carcinogenesis have remained largely unknown, however.

Gastric cancer is the third most prevalent cancer worldwide and is the second leading cause of cancer-related deaths (>1 million deaths

Abbreviations: ALK, anaplastic lymphoma kinase; cDNA, complementary DNA; ERK, extracellular signal-regulated kinase; MAPK, mitogen-activated protein kinase; NSCLC, non-small cell lung cancer.

per year) (7). Whereas the diagnosis of gastric cancer has become more sensitive and reliable with the implementation of gastrointestinal endoscopy, unresectable gastric cancer remains mostly intractable. Given the promising efficacy of an inhibitor of the anaplastic lymphoma kinase (ALK) in the treatment of non-small cell lung cancer (NSCLC) positive for the EML4-ALK fusion protein (8,9) and of a BRAF inhibitor in the treatment of melanoma positive for BRAF mutations (10), the identification of additional oncogenes on which cancer cells are dependent should provide a basis for the targeting of such genes in the development of anticancer agents with improved efficacy (11).

We have now adopted the OCUM-1 cell line of scirrhous-type gastric cancer to screen for transforming genes. A retroviral complementary DNA (cDNA) expression library was constructed from the OCUM-1 cells and was then used for a focus formation assay with mouse 3T3 fibroblasts. We thereby identified a transforming mutant of MAP2K1 and further showed that OCUM-1 cells are dependent on MAP2K1 activity for growth. Deep sequencing of *MAP2K1* cDNAs among a total of 171 cancer specimens and cell lines further identified known and novel activating mutations of MAP2K1.

Materials and methods

Cell lines and specimens

Three cell lines of scirrhous-type gastric cancer (OCUM-1, KATOIII and NUGC-4) were obtained from the Japanese Collection of Research Bioresources (Osaka, Japan), and HEK293 and 3T3 cell lines were obtained from American Type Culture Collection (Manassas, VA). These cells were maintained in Dulbecco's modified Eagle's medium-F12 (Invitrogen, Carlsbad, CA) supplemented with 10% fetal bovine serum and 2 mM L-glutamine (both from Invitrogen). Where indicated, cells were incubated with 20 nM of the MAP2K1 inhibitor AZD6244 (Selleckchem, Houston, TX). Total RNA was extracted from cell lines and cancer specimens with an RNeasy Mini Kit (Qiagen, Valencia, CA) and was subjected to reverse transcription with an oligo(deoxythymidine) primer. Written informed consent was obtained from the subjects who provided cancer specimens, and the study was approved by the human ethics committee of Jichi Medical University.

Focus formation assay

Recombinant ecotropic retroviruses for expression of OCUM-1 cell cDNAs were constructed as described previously (8). Mouse 3T3 cells were infected with the retroviral library at a multiplicity of infection of 0.1 infectious particle per cell, and the cells were then cultured for 2–3 weeks in Dulbecco's modified Eagle's medium-F12 medium supplemented with 5% calf serum (Invitrogen). Genomic DNA was extracted from transformed foci and was subjected to PCR with 5'-PCR primer IIA (Clontech, Mountain View, CA) in order to rescue retrovirus inserts. The nucleotide sequence of rescued cDNAs was determined with a Sanger sequencer.

Functional assay of MAP2K1

The cDNAs for wild-type or mutant forms of MAP2K1 were inserted into the retroviral plasmid pMXS (12), and the modified plasmids were then used to generate recombinant ecotropic retroviruses. Each virus was used to infect 3T3 cells, which were subsequently subjected to a focus formation assay as well as a tumorigenicity assay with nude mice, the latter of which was approved by the institutional review board for animal experiments in Jichi Medical University. The viral plasmids were also used to transfect HEK293 cells by the calcium phosphate method, and the transfected cells were subsequently subjected to immunoblot analysis with antibodies to phosphorylated or total forms of extracellular signal-regulated kinase (ERK) (both from Cell Signaling Technology).

Multiplex deep sequencing of MAP2K1 cDNAs

The entire open reading frame of *MAP2K1* cDNA was amplified by PCR with the primers 5'-AGCGGATCCCGGGTCCAAAATGCC-3' and 5'-CTTCTCGAGCACTTAGACGCCAGCAGC-3' from total cDNAs of 171 cancer specimens or cell lines, and the amplification products were fragmented and then subjected to deep sequencing with a Genome Analyzer IIx (GAIIx; Illumina, San Diego, CA) for 76 bases from both ends of each fragment with the paired-end sequencing option. We modified the paired-end adaptors (Illumina) for a multiplex reaction so that an 'N₁N₂' or 'X₂X₁' doublet was added to the 5' or 3' end, respectively, of cDNA fragments (N₁ and N₂ are any bases